

ELECTRONIC SUPPLEMENTARY INFORMATION

Molecular design principles of ionic liquids with a sulfonyl fluoride moiety

David J. Siegel,^{a,†} Grace I. Anderson,^{a,†} Noah Cyr,^a Daniel S. Lambrecht,^a Matthias Zeller,^c Patrick C. Hillesheim,*^b and Arsalan Mirjafari*^a

^a*Department of Chemistry and Physics, Florida Gulf Coast University, Fort Myers, Florida 33965, USA. Email: amirjafari@fgcu.edu*

^b*Department of Chemistry and Physics, Ave Maria University, Ave Maria, Florida 34142, USA. Email: patrick.hillesheim@avemaria.edu*

^c*Department of Chemistry, Purdue University, West Lafayette, Indiana 47907, USA.*

* These authors contributed equally to this work.

1. Materials and instrumentation

All commercial chemicals were used as received unless otherwise noted. Extra dry solvents over molecular sieves were purchased from Acros Organics. ^1H , ^{13}C and ^{19}F NMR were performed on a JEOL 400 MHz NMR at 295 K. Chemical shifts (δ) are quoted in parts per million (ppm) and referenced to the appropriate NMR solvent residual peaks. ESI-MS analyses were performed by flow-injection on a Thermo Scientific ion trap mass spectrometer using HPLC grade acetonitrile and data were collected in positive and negative ion mode. Melting points and glass transition temperatures were measured using a TA Q100 differential scanning calorimeter calibrated using indium (melting point) and sapphire (heat capacity) references with a heating and subsequent cooling rate of 2 °C/min. Thermogravimetric analyses were performed on a TA instrument TGA Q500 under nitrogen flow using an aluminum pan. The samples were heated at 2 °C/min. Dynamic and kintetic viscosity, and density were measured by Stabinger Viscometer SVM 3001 from Anton-Paar. SC-XRD experiments were carried out with Mo or Cu- $\text{K}\alpha$ radiation using Bruker AXS D8 Quest diffractometer with Photon100 or PhotonII charge-integrating pixel array detectors (CPAD). Absorption was corrected for by multi-scan methods, SADABS or TWINABS.¹ Additional details are given in the XRD section can be found in Section 5 (*vide infra*).

2. Differential scanning calorimetry

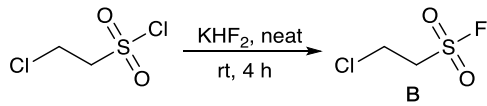
In his work, glass transition temperatures are reported as the transition from an amorphous solid state to the isotropic liquid state. Samples (5–10 mg) were loaded into sealed DSC aluminum pans and heated to 120 °C for 10 min to remove any water absorbed from the environment. The samples were then cooled to –50 °C and heated at a ramp rate of 2 °C/min to 150 °C. Their glass transition temperatures are reported midpoints of phase transitions as calculated by the analysis software (TA Universal Analysis). Ten scans were carried out to identify the correct phase transitions by observing three overlapping cycles. All measurements were carried out under a nitrogen atmosphere and were reproducible to within ±1 °C, although varying the thermal history of the sample produced variations in the transition temperatures, a phenomenon often observed in ionic liquids.

3. Experimental section and structural characterization

Preparation of 2-chloroethanesulfonyl fluoride. 2-Chloroethanesulfonyl fluoride ($\text{ClCH}_2\text{CH}_2\text{SO}_2\text{F}$) is readily prepared *via* the reaction between a saturated potassium bifluoride (KHF_2) solution (*Warning! Potassium bifluoride solutions are hazardous and will etch glassware*) and 2-chloroethanesulfonyl chloride, as reported by Sharpless *et al.*² Briefly, in a 250 mL round-bottom flask, a Teflon-coated egg-shaped stir bar, deionized water (93 mL) and KHF_2 (30 g, 0.38 mol, 98% purity, Alfa Aesar™) were added. The solution was vigorously stirred for 2 h at ambient temperature to form a near saturated KHF_2 solution. Then, 2-chloroethanesulfonyl chloride (26.9 g, 0.15 mol, >95% purity, TCI Chemicals) was added in one portion to the solution while stirring. The biphasic solution was stirred vigorously to form an emulsion for 2 h at ambient temperature. Using a 250 mL glass separatory funnel, the lower phase was drained into a 250 mL glass Erlenmeyer flask, dried over anhydrous MgSO_4 (3 g), and filtered, yielding 2-chloroethanesulfonyl fluoride (Schemes S1 and S2, compound **B**) in quantitative yield. Three 25 mL portions of dichloromethane (3 x 25 mL) was used to wash the reaction vessel and to extract the upper aqueous phase. The combined organic phase was washed with 25 mL of brine, dried over 3 g of anhydrous MgSO_4 , and filtered through a sintered glass Buchner funnel.

Characterization data consisted of ^1H and ^{19}F NMR.

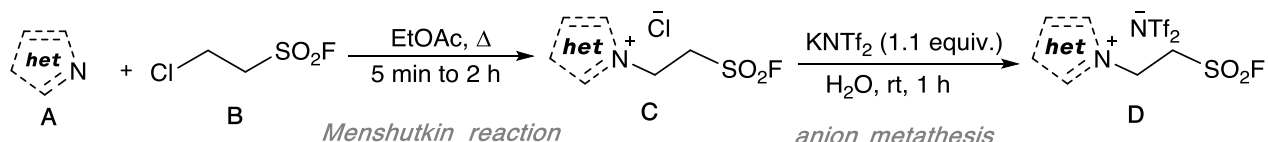
Preparation of KNTf_2 . The potassium salt of $(\text{CF}_3\text{SO}_2)_2\text{N}^-$ ($[\text{Tf}_2\text{N}]^-$) was prepared by neutralizing an 80% (w/w) aqueous solution of the corresponding acid HTf_2N (IoLiTec -



Scheme S1. On-water preparation of 2-chloroethanesulfonyl fluoride (**B**).

Ionic Liquids Technologies GmbH) with aqueous KOH, followed by removal of water under the reduced pressure at 80 °C.

Menshutkin reaction. As shown in scheme S2, equimolar amounts of heterocycles **A** and 2-chloroethanesulfonyl fluoride **2** were dissolved separately in EtOAc and were added to a 250 mL round-bottom flask equipped with a Teflon-coated magnetic stir bar. The reaction mixture was vigorously stirred at ambient temperature for 2 h. Except, when **A** is 1-methyl-5-nitroimidazole, 1,2-dimethyl-5-nitroimidazole, and PyFluor, then reflux conditions are required. Some products were formed instantly upon the addition of **A** and **B** (see Figure S1; **A**: 1-methylimidazole). The products were collected *via* filtration, were washed with cold EtOAc and were dried *in vacuo* to obtain the chloride analog of the products (**C**) as white crystalline solids (100% isolated yields). Characterization data consisted of ¹H, ¹³C and ¹⁹F NMR.



Scheme S2. Two-step synthesis of the sulfonyl fluoride-based ionic liquids.

Anion metathesis. Next, 1.0 equiv. of the **C** salts and KNTf₂ (1.1 equiv.) were dissolved in deionized water separately and then added to a 250 mL round-bottomed flask equipped with a magnetic stir bar and glass stopper. The mixture was stirred at ambient temperature for 2 h, forming two distinct phases. The lower layer was separated and washed with water three times. The solvent was removed under reduced pressure, yielding a residue constituting the product IL. This was then dried by heating *in vacuo* for 8 h at 50 °C, yielded IL **3** products in quantitative yields (Scheme S2). Characterization data consisted of ¹H, ¹³C and ¹⁹F NMR as well as ESI-MS.

 3a	¹ H NMR (400 MHz, DMSO-D6) δ 9.21 (s, 1H), 7.83 (d, <i>J</i> = 1.8 Hz, 1H), 7.74 (d, <i>J</i> = 1.7 Hz, 1H), 4.82 (t, <i>J</i> = 6.2 Hz, 2H), 4.67 (t, <i>J</i> = 6.3 Hz, 2H), 3.89 (s, 3H). ¹⁹ F NMR (376 MHz, DMSO-D6) δ -78.7. ¹³ C NMR (101 MHz, DMSO-D6) δ 137.4, 124.3, 123.8, 122.7, 121.1, 117.9, 114.7, 49.5, 42.8, 35.9. MS (EI): <i>m/z</i> 193.8 (M = C ₆ H ₁₀ FN ₂ O ₂ S ⁺ , calcd. 193.0).
 3b	¹ H NMR (400 MHz, CD ₃ OD) δ 7.59 (d, <i>J</i> = 2.3 Hz, 1H), 7.51 (d, <i>J</i> = 2.1 Hz, 1H), 3.28 (t, <i>J</i> = 1.6 Hz, 2H), 4.82 (t, <i>J</i> = 6.2 Hz, 2H), 4.67 (q, <i>J</i> = 6.3 Hz, 2H), 3.82 (s, 3H). ¹⁹ F NMR (376 MHz, CD ₃ OD) δ -80.6. ¹³ C NMR (101 MHz, CD ₃ OD) δ 123.9, 122.0, 121.1, 117.9, 114.7, 49.2, 48.8, 35.3, 9.3. MS (EI): <i>m/z</i> 207.8 (M = C ₇ H ₁₂ FN ₂ O ₂ S ⁺ , calcd. 207.1).
 3c	¹ H NMR (400 MHz, CD ₃ OD) δ 9.43 (s, 1H), 8.95 (s, 1H), 4.93 (t, <i>J</i> = 6.1 Hz, 2H), 4.47-4.44 (m, 2H), 4.22 (s, 3H). ¹⁹ F NMR (376 MHz, CD ₃ OD) δ -79.8. ¹³ C NMR (101 MHz, CD ₃ OD) δ 125.6, 122.8, 119.6, 116.4, 50.1, 49.0, 38.3. MS (EI): <i>m/z</i> 238.5 (M = C ₆ H ₉ FN ₃ O ₄ S ⁺ , calcd. 238.0).

	¹ H NMR (400 MHz, CD ₃ OD) δ 8.91 (s, 1H), 4.93 (t, <i>J</i> = 6.2 Hz, 2H), 4.42 (t, <i>J</i> = 6.4 Hz, 2H), 4.12 (s, 3H), 2.84 (s, 3H). ¹⁹ F NMR (376 MHz, CD ₃ OD) δ -80.6. ¹³ C NMR (101 MHz, CD ₃ OD) δ 150.7, 125.2, 122.8, 119.6, 116.4, 50.1, 44.4, 36.1, 10.8. MS (EI): <i>m/z</i> 252.4 (M = C ₇ H ₁₁ FN ₃ O ₄ S ⁺ , calcd. 252.0).
	¹ H NMR (400 MHz, CD ₃ OD) δ 10.95 (s, 1H), 10.01 (s, 1H), 5.93 (t, <i>J</i> = 6.2 Hz, 2H), 5.40 (t, <i>J</i> = 6.4 Hz, 2H), 5.16 (s, 3H). ¹⁹ F NMR (376 MHz, CD ₃ OD) δ -80.6. ¹³ C NMR (101 MHz, CD ₃ OD) δ 144.7, 143.5, 142.8, 124.6, 121.4, 118.2, 115.0, 48.9, 48.4. MS (EI): <i>m/z</i> 194.6 (M = C ₅ H ₉ FN ₃ O ₂ S ⁺ , calcd. 194.0).
	¹ H NMR (400 MHz, CD ₃ OD) δ 9.09 (d, <i>J</i> = 6.4 Hz, 2H), 8.69 (t, <i>J</i> = 7.9 Hz, 1H), 8.18 (t, <i>J</i> = 7.0 Hz, 2H), 5.25 (t, <i>J</i> = 6.3 Hz, 2H), 4.62 (t, <i>J</i> = 6.2 Hz, 2H). ¹⁹ F NMR (376 MHz, CD ₃ OD) δ -80.6. ¹³ C NMR (101 MHz, CD ₃ OD) δ 148.4, 146.8, 129.7, 126.0, 122.8, 119.6, 116.4, 56.2, 50.8. MS (EI): <i>m/z</i> 190.5 (M = C ₇ H ₉ FNO ₂ S ⁺ , calcd. 190.0).
	¹ H NMR (400 MHz, CD ₃ OD) δ 9.07 (d, <i>J</i> = 6.4 Hz, 2H), 8.67 (d, <i>J</i> = 8.0 Hz, 1H), 8.17 (t, <i>J</i> = 7.0 Hz, 2H), 5.23 (t, <i>J</i> = 6.3 Hz, 2H), 4.60 (t, <i>J</i> = 6.2 Hz, 2H); ¹⁹ F NMR (376 MHz, CD ₃ OD) δ -80.6. ¹³ C NMR (101 MHz, CD ₃ OD) δ 147.0, 145.5, 128.3, 127.3, 124.6, 121.4, 118.3, 115.1, 54.8, 49.5. MS (EI): <i>m/z</i> 205.8 (M = C ₇ H ₁₂ FN ₂ O ₂ S ⁺ , calcd. 205.0).
	¹ H-NMR (400 MHz, CD ₃ OD) δ 8.86 (dd, <i>J</i> = 6.1, 2H), 7.70 (dd, <i>J</i> = 5.9, 2H), 5.49 (s, 6H), 4.00-3.93 (m, 4H). ¹⁹ F NMR (376 MHz, CD ₃ OD) δ -80.6. ¹³ C NMR (101 MHz, CD ₃ OD) δ 157.8, 142.9, 125.6, 122.4, 119.2, 116.1, 108.7, 107.9, 66.6, 51.8, 49.3, 49.1. MS (EI): <i>m/z</i> 233.4 (M = C ₉ H ₁₄ FN ₂ O ₂ S ⁺ , calcd. 233.1).
	¹ H NMR (400 MHz, DMSO-D6) δ 8.80-8.78 (m, 1H), 8.18-8.17 (m, 2H), 7.83-7.80 (m, 1H), 4.08 (q, <i>J</i> = 5.9 Hz, 2H), 3.93 (t, <i>J</i> = 6.3 Hz, 2H). ¹⁹ F NMR (376 MHz, DMSO-D6) δ -78.8, -148.5. ¹³ C NMR (101 MHz, DMSO-D6) δ 124.3, 121.1, 117.9, 114.7, 79.2, 78.9, 78.5. MS (EI): <i>m/z</i> 272.2 (M = C ₇ H ₈ F ₂ NO ₄ S ⁺ , calcd. 272.0).
	¹ H NMR (400 MHz, DMSO-D6) δ 3.44 (s, 2H), 2.90 (s, 2H), 2.74 (s, 3H), 1.92 (d, <i>J</i> = 43.9 Hz, 6H). ¹⁹ F NMR (376 MHz, DMSO-D6) δ -78.6. ¹³ C NMR (101 MHz, DMSO-D6) δ 124.8, 121.6, 118.4, 115.2, 54.9, 40.7, 40.5, 39.4, 23.4. MS (EI): <i>m/z</i> 196.8 (M = C ₇ H ₁₅ FNO ₂ S ⁺ , calcd. 196.1).
	¹ H-NMR (400 MHz, DMSO-D6) δ 4.04 (s, 2H), 3.70 (s, 2H), 3.41 (s, 2H), 3.31-3.29 (m, 2H), 3.15 (s, 2H), 2.91 (s, 3H). ¹⁹ F NMR (376 MHz, DMSO-D6) δ -78.7. ¹³ C NMR (101 MHz, DMSO-D6) δ 124.8, 121.6, 118.4, 115.2, 63.9, 53.1. MS (EI): <i>m/z</i> 212.5 (M = C ₇ H ₁₅ FNO ₃ S ⁺ , calcd. 212.1).
	¹ H NMR (400 MHz, DMSO-D6) δ 9.15 (s, 1H), 7.78 (d, <i>J</i> = 1.4 Hz, 1H), 7.70 (d, <i>J</i> = 1.4 Hz, 1H), 4.78 (d, <i>J</i> = 6.1 Hz, 2H), 4.63 (d, <i>J</i> = 6.1 Hz, 2H), 3.85 (s, 3H). ¹⁹ F NMR (376 MHz, DMSO-D6) δ -78.5, -117.3. ¹³ C NMR (101 MHz, DMSO-D6) δ 137.9, 124.4, 123.2, 120.1, 119.7, 119.4, 117.2, 116.9, 116.5, 114.7, 114.4, 114.0, 111.8, 111.5, 50.0, 49.8, 43.3, 36.5. MS (EI): <i>m/z</i> 193.8 (M = C ₆ H ₁₀ FN ₂ O ₂ S ⁺ , calcd. 193.0).

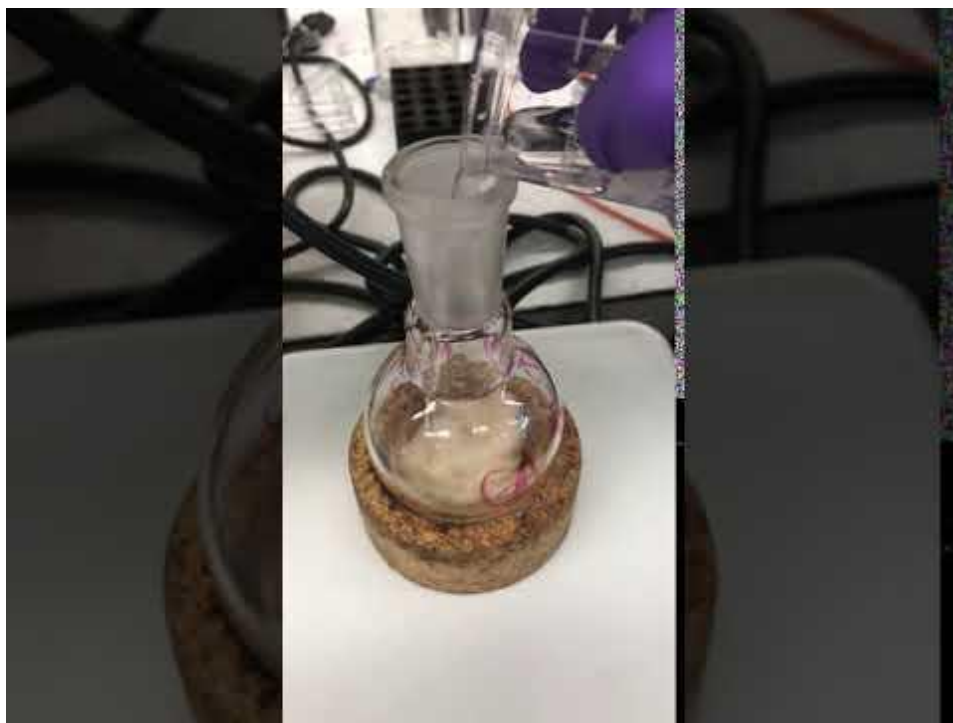


Figure S1. Instant formation of the chloride analog of the IL **3j**.

4. Thermophysical data

Table S1. Dynamic and kinetic visosity, and density data of IL **3a**.

Cell Temp. (°C) ± 0.1 °C	Dyn. Visc. (mPa·s)	Kin. Visc. (mm²/s)	Density (g/cm³) ± 0.0005 g/cm³
20.000	1081.9	645.37	1.67640
25.000	715.12	427.91	1.67121
30.000	487.98	292.87	1.66620
35.000	343.46	206.75	1.66121
40.001	250.29	151.13	1.65610
45.001	186.00	112.65	1.65110
50.001	141.45	85.928	1.64611
55.000	109.74	66.862	1.64123
60.000	86.680	52.972	1.63634
65.001	69.608	42.667	1.63143
69.999	56.776	34.908	1.62646
75.000	46.856	28.895	1.62159
80.001	39.054	24.156	1.61673

The viscosity data for **3a** fits to the Vogel-Fulcher-Tamman (VFT) expression (Equation 1) while the density data were fit to a simple quadratic expression (Equation 2) in temperature.

$$\text{Equation 1} \quad \eta \text{ (mPa.s)} = \eta_\infty \exp\left(\frac{k}{T - T_0}\right)$$

$$\text{Equation 2} \quad \rho \text{ (g/cm³)} = D_1 + D_2 T(K) + D_3 T(K)^2$$

5. Crystallographic data

General Procedures. Single crystals data of samples **3c** and **3f** were collected on a Bruker Quest diffractometer with kappa geometry, a Cu K α wavelength ($\lambda = 1.54178 \text{ \AA}$) I- μ -S microsource X-ray tube, laterally graded multilayer (Goebel) mirror single crystal for monochromatization, a Photon II area detector and an Oxford Cryosystems low temperature device. Examination and data collection were performed at 150 K. Single crystals data of sample **3b** were collected on a Bruker AXS D8 Quest diffractometer with a Mo K α wavelength ($\lambda = 0.71073 \text{ \AA}$) sealed tube X-ray source, a curved graphite crystal for monochromatization, a Photon100 area detector and an Oxford Cryosystems low temperature device. Examination and data collection were performed at 150 K. Single crystals data of sample **3a-BETI** were collected on a Bruker AXS D8 Quest Eco diffractometer with a Mo K α wavelength ($\lambda = 0.71073 \text{ \AA}$) sealed tube X-ray source, a curved graphite crystal for monochromatization, a Photon II area detector and an Oxford Cryosystems low temperature device. Examination and data collection were performed at 100 K. For all samples, data were collected, reflections were indexed and processed, and the files scaled and corrected for absorption using APEX3³ and SADABS or TWINABS.¹ The space groups were assigned and the structures were solved by direct methods using XPREP within the SHELXTL suite of programs⁴ and refined by full matrix least squares against F^2 with all reflections using Shelxl2018⁵ using the graphical interfaces Shelxle⁶ and/or Olex.⁷ H atoms were positioned geometrically and constrained to ride on their parent atoms. C-H bond distances were constrained to 0.95 \AA for aromatic and alkene C-H moieties, and to 0.99 and 0.98 \AA for aliphatic CH₂ and CH₃ moieties, respectively. Methyl H atoms were allowed to rotate but not to tip to best fit the experimental electron density. U_{iso}(H) values were set to a multiple of U_{eq}(C) with 1.5 for CH₃ and 1.2 for C-H and CH₂ units, respectively.

Sample **3b** exhibits disorder. The imidazole ring is disordered by a 180° rotation. The SO₂F unit was excluded from the disorder, but the disorder extends to the neighboring anion, inducing slight shifts of oxygen and fluorine atoms. Disorder was extended to the entire anion. The same occupancy ratio was used for both anion and cation. ADPs of the atoms C7A and C7B, C8A and C8B and C11A and C11B (of the cation) and of atoms C10A and C10B, C11A and C11B, F5 and F5B, F6 and F6B, and F7 and F7B (of the anion) were constrained to be pairwise identical. C7A and C7B were also constrained to have identical coordinates. Major and minor disordered moieties were restrained to have similar geometries (SAME restraints of Shelxl). U^{ij} components of ADPs for disordered atoms closer to each other than 2.0 \AA were restrained to be similar. Subject to these conditions the occupancy ratio refined to 0.8832(19) to 0.1168(19).

For sample **3c**, the crystal under investigation was found to be non-merohedrally twinned. The orientation matrices for the two components were identified using the program Cell_Now, with the two components being related by a 180° rotation around the reciprocal c-axis. The two components were integrated using Saint and corrected for absorption using twinabs, resulting in the following statistics:

4440 data (1528 unique) involve domain 1 only, mean I/sigma 16.9
4265 data (1459 unique) involve domain 2 only, mean I/sigma 8.7
20720 data (6010 unique) involve 2 domains, mean I/sigma 11.0
28 data (28 unique) involve 3 domains, mean I/sigma 6.6

The exact twin matrix identified by the integration program was found to be:

-1.00001 0.00029 -0.00018
-0.00089 -1.00000 0.00125
0.09591 0.00147 1.00001

The structure was solved using direct methods with only the non-overlapping reflections of component 1. The structure was refined using the hklf 5 routine with all reflections of component 1 (including the

overlapping ones), resulting in a BASF value of 0.162(1). The R_{int} value given is for all reflections and is based on agreement between observed single and composite intensities and those calculated from refined unique intensities and twin fractions.⁸

For sample **3f**, the structure is metrically monoclinic C-centered and is twinned by pseudo-merohedry by this symmetry. Application of the twin transformation matrix -1 0 0, 0 -1 0, 0 -1 1 yielded a twin ratio of 0.4953(6) to 0.5047(6).

The anion of sample **3a-BETI** exhibits extensive disorder. The entire anion exhibits two-fold disorder, and half the major moiety is further split into an additional two segments. Equivalent disordered moieties were restrained to have similar geometries. U^{ij} components of ADPs for disordered atoms closer to each other than 2.0 Angstrom were restrained to be similar. Subject to these conditions the occupancy rates refined to 0.8766(17) for the major “A” moiety, to 0.1234(17) for the minor “C” moiety, and to 0.591(2) and 0.285(2) for the further split major moiety (“A” and “B”, respectively).

Complete crystallographic data, in CIF format, have been deposited with the Cambridge Crystallographic Data Centre. CCDC Numbers 2032772 (**3b**), 2032771 (**3c**), 2032773 (**3f**), and 2032774 (**3a-BETI**), contain the supplementary crystallographic data for this paper. These data can be obtained free of charge from The Cambridge Crystallographic Data Centre via www.ccdc.cam.ac.uk/data_request/cif.

Table S2. Relative percentages of interactions obtained from the fingerprint plots of the four crystals.

3a-BETI					
Cation	H···All	H···F F···H	H···O O···H	H···N N···H	H···H
	63.4	38.0	34.9	2.2	0.9
	F···All	F···F	F···O	F···H	
	9.0	4.7	0.2	4.1	
	O···All	O···F	O···O	O···H	
	19.7	8.5	2.7	8.5	
	N···All	N···F	N···O		
	2.4	1.7	0.7		
	C···All	C···F	C···O		
	5.5	3.1	2.4		
3b					
Cation	H···All	H···F F···H	H···O O···H	H···N N···H	H···H
	67.1	27.8	39.1	2.3	9.3
	F···All	F···F	F···O	F···H	
	7.6	4.3	1.1	2.3	
	O···All	O···F	O···O	O···H	
	17.9	4.5	3.1	9.2	
	N···All	N···F	N···O		
	2.6	1.2	1.2		
	C···All	C···F	C···O		
	4.7	3.2	1.0		
3c					
Cation	H···All	H···F F···H	H···O O···H	H···N N···H	H···H
	48.2	14.9	47.7	0.4	3.4
	F···All	F···F	F···O	F···H	
	7.8	2.7	1.8	3.1	
	O···All	O···F	O···O	O···H	
	34.5	15.3	4.0	15.2	

	N···All	N···F	N···O		
	4.4	1.9	1.3		
	C···All	C···F	C···O		
	5.1	1.8	2.0		
3f					
Cation C	H···All	H···F F···H	H···O O···H	H···N N···H	H···H
	59.3	25.4	43.0	-	4.2
	F···All	F···F	F···O	F···H	
	8.4	3.6	0.7	3.3	
	O···All	O···F	O···O	O···H	
	20.7	8.9	1.6	10.1	
	N···All	N···F	N···O		
	1.3	0.9	0.4		
	C···All	C···F	C···O		
	10.3	5.7	4.6		

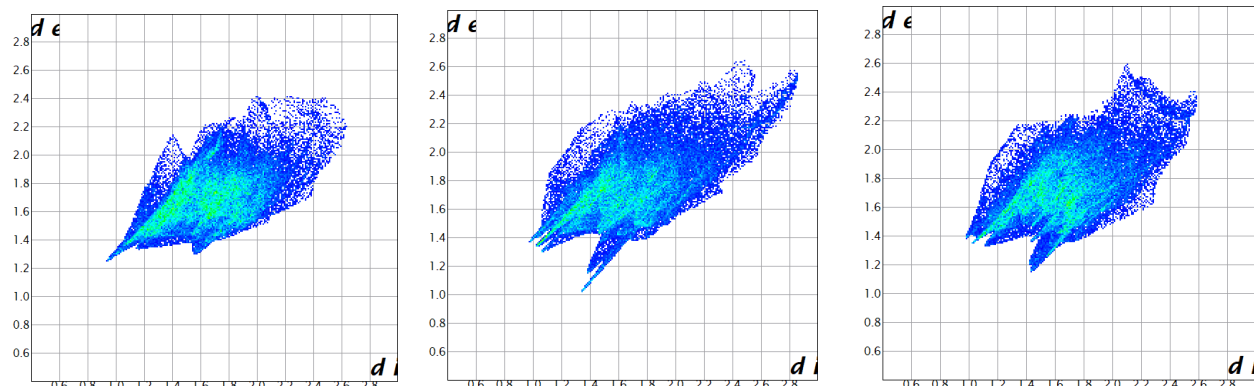


Figure S2. From left to right: Fingerprints of cations A, B and D in IL 3f.

Table S3. Crystal data of **3b**

Chemical formula	$C_7H_{12}FN_2O_2S \cdot C_2F_6NO_4S_2$
M_r	487.40
Crystal system, space group	Triclinic, $P\bar{1}$
Temperature (K)	150
a, b, c (Å)	8.7261 (7), 10.1432 (10), 10.1921 (11)
α, β, γ (°)	86.557 (4), 88.953 (4), 80.564 (3)
V (Å ³)	888.27 (15)
Z	2
Radiation type	Mo $K\alpha$
μ (mm ⁻¹)	0.52
Crystal size (mm)	0.48 × 0.32 × 0.29
Data collection	
Diffractometer	Bruker AXS D8 Quest diffractometer with CMOS Photon100 detector
Absorption correction	Multi-scan SADABS 2016/2: Krause, L., Herbst-Irmer, R., Sheldrick G.M. & Stalke D., J. Appl. Cryst. 48 (2015) 3-10
T_{min}, T_{max}	0.703, 0.747
No. of measured, independent and observed [$I > 2\sigma(I)$] reflections	29669, 6786, 5686
R_{int}	0.028
$(\sin \theta/\lambda)_{\max}$ (Å ⁻¹)	0.771
Refinement	
$R[F^2 > 2\sigma(F^2)], wR(F^2), S$	0.036, 0.103, 1.03
No. of reflections	6786
No. of parameters	423
No. of restraints	786
H-atom treatment	H-atom parameters constrained
$\Delta\rho_{\max}, \Delta\rho_{\min}$ (e Å ⁻³)	0.46, -0.35

Table S4. Crystal data of **3c**

Chemical formula	$C_6H_9FN_3O_4S \cdot C_2F_6NO_4S_2$
M_r	518.37
Crystal system, space group	Monoclinic, $P2_1/c$
Temperature (K)	150
a, b, c (Å)	7.9991 (7), 14.4267 (15), 15.7810 (16)
β (°)	91.373 (4)
V (Å ³)	1820.6 (3)
Z	4
Radiation type	Mo $K\alpha$
μ (mm ⁻¹)	0.53
Crystal size (mm)	0.41 × 0.16 × 0.04
Data collection	
Diffractometer	Bruker AXS D8 Quest diffractometer with PhotonII charge-integrating pixel array detector (CPAD)
Absorption correction	Multi-scan TWINABS 2012/1: Krause, L., Herbst-Irmer, R., Sheldrick G.M. & Stalke D. (2015). <i>J. Appl. Cryst.</i> 48 3-10.
T_{\min}, T_{\max}	0.598, 0.747
No. of measured, independent and observed [$I > 2\sigma(I)$] reflections	6289, 6289, 4834
R_{int}	0.060
$(\sin \theta/\lambda)_{\max}$ (Å ⁻¹)	0.769
Refinement	
$R[F^2 > 2\sigma(F^2)], wR(F^2), S$	0.054, 0.141, 1.04
No. of reflections	6289
No. of parameters	273
H-atom treatment	H-atom parameters constrained
$\Delta\rho_{\max}, \Delta\rho_{\min}$ (e Å ⁻³)	0.48, -0.45

Table S5. Crystal data of **3f**.

Chemical formula	<chem>C2F6NO4S2.C7H9FNO2S</chem>
M_r	470.36
Crystal system, space group	Triclinic, $P\bar{1}$
Temperature (K)	150
a, b, c (Å)	12.029 (3), 15.417 (3), 19.656 (6)
α, β, γ (°)	66.957 (13), 88.617 (16), 86.55 (2)
V (Å ³)	3348.3 (16)
Z	8
Radiation type	Mo $K\alpha$
μ (mm ⁻¹)	0.55
Crystal size (mm)	0.35 × 0.31 × 0.09
Data collection	
Diffractometer	Bruker AXS D8 Quest diffractometer with PhotonII charge-integrating pixel array detector (CPAD)
Absorption correction	Multi-scan <i>SADABS</i> 2016/2: Krause, L., Herbst-Irmer, R., Sheldrick G.M. & Stalke D., <i>J. Appl. Cryst.</i> 48 (2015) 3-10
T_{\min}, T_{\max}	0.629, 0.747
No. of measured, independent and observed [$I > 2\sigma(I)$] reflections	56242, 22814, 17154
R_{int}	0.069
$(\sin \theta / \lambda)_{\max}$ (Å ⁻¹)	0.771
Refinement	
$R[F^2 > 2\sigma(F^2)], wR(F^2), S$	0.043, 0.113, 1.02
No. of reflections	22814
No. of parameters	974
H-atom treatment	H-atom parameters constrained
$\Delta\rho_{\max}, \Delta\rho_{\min}$ (e Å ⁻³)	0.64, -0.49

Table S6. Crystal data of **3a—BETI**.

Chemical formula	$C_6H_{10}FN_2O_2S \cdot 1.141(C_{3.506}F_{8.766}N_{0.877}O_{3.506}S_{1.753})$
M_r	573.39
Crystal system, space group	Monoclinic, $P2_1/c$
Temperature (K)	100
a, b, c (Å)	9.8011 (3), 11.0925 (3), 18.3728 (6)
β (°)	97.261 (1)
V (Å ³)	1981.45 (10)
Z	4
Radiation type	Mo $K\alpha$
μ (mm ⁻¹)	0.51
Crystal size (mm)	0.31 × 0.21 × 0.08
Data collection	
Diffractometer	Bruker AXS D8 Quest ECO diffractometer with a Photon II charge-integrating pixel array detector (CPAD)
Absorption correction	Multi-scan <i>SADABS2016/2</i> (Bruker,2016/2) was used for absorption correction. wR2(int) was 0.0784 before and 0.0558 after correction. The Ratio of minimum to maximum transmission is 0.8944. The $\lambda/2$ correction factor is Not present.
T_{\min}, T_{\max}	0.668, 0.747
No. of measured, independent and observed [$I > 2\sigma(I)$] reflections	83794, 9618, 7876
R_{int}	0.032
(sin θ/λ) _{max} (Å ⁻¹)	0.834
Refinement	
$R[F^2 > 2\sigma(F^2)], wR(F^2), S$	0.049, 0.134, 1.10
No. of reflections	9618
No. of parameters	581
No. of restraints	1223
H-atom treatment	H-atom parameters constrained
$\Delta\rho_{\max}, \Delta\rho_{\min}$ (e Å ⁻³)	0.64, -0.62

6. Computational data

Table S7. Computationally predicted bond lengths for **3b** at the solvent dielectric constant $\varepsilon_r = 6$ employing the C-PCM treatment.

Bond	Start	End	Order	Length (Å)
Bond 1	H1	C1	1	1.0813
Bond 2	H2	C2	1	1.08108
Bond 3	C1	C2	2	1.35097
Bond 4	C1	N2	1	1.38152
Bond 5	C2	N1	1	1.37647
Bond 6	F3	C8	1	1.32412
Bond 7	F2	C8	1	1.3344
Bond 8	O6	S3	2	1.46243
Bond 9	H10	C6	1	1.09231
Bond 10	O5	S3	2	1.46097
Bond 11	H11	C7	1	1.09403
Bond 12	C8	F4	1	1.33059
Bond 13	C8	S2	1	1.86645
Bond 14	N2	C6	1	1.45574
Bond 15	N2	C3	1	1.34323
Bond 16	S3	N3	1	1.60861
Bond 17	S3	C9	1	1.86534
Bond 18	H4	C4	1	1.09028
Bond 19	N1	C4	1	1.45608
Bond 20	N1	C3	1	1.33266
Bond 21	C6	C7	1	1.52554
Bond 22	C6	H9	1	1.09302
Bond 23	F1	S1	1	1.63692
Bond 24	C7	H12	1	1.09913
Bond 25	C7	S1	1	1.77497
Bond 26	N3	S2	1	1.60104
Bond 27	C4	H5	1	1.09412
Bond 28	C4	H3	1	1.09059
Bond 29	C3	C5	1	1.47825
Bond 30	F6	C9	1	1.32962
Bond 31	S2	O4	2	1.45997
Bond 32	S2	O3	2	1.46702
Bond 33	S1	O2	2	1.44427
Bond 34	S1	O1	2	1.44794
Bond 35	C9	F5	1	1.33159
Bond 36	C9	F7	1	1.32694
Bond 37	C5	H6	1	1.09575
Bond 38	C5	H7	1	1.09125
Bond 39	C5	H8	1	1.09442

Table S8. Computationally predicted three-dimensional coordinates for **3b** at the solvent dielectric constant $\varepsilon_r = 6$ employing the C-PCM treatment.

Atom	Coordinates (Å)		
	X	Y	Z
1 S	-4.70955365	0.730440521	0.987014325
2 F	-5.84482111	0.417644527	-0.15001264
3 O	-5.00372736	-0.17416561	2.078651762
4 O	-4.7133357	2.163870392	1.16357057
5 N	-0.01339999	-2.61843426	-0.3684859
6 N	-1.9854283	-1.77539132	-0.5730775
7 C	-1.43431633	-1.82506244	-1.83894225
8 H	-1.97205037	-1.4707278	-2.70755765
9 C	-0.19737249	-2.3518308	-1.70629728
10 H	0.575673047	-2.5477303	-2.43619558
11 C	-1.09826818	-2.25434475	0.314506146
12 C	1.180940678	-3.21211164	0.215704184
13 H	1.417765152	-2.69515612	1.146331162
14 H	2.003942745	-3.06706797	-0.4845373
15 H	1.011252784	-4.27706191	0.400569291
16 C	-1.26241996	-2.38368747	1.777906055
17 H	-1.19716778	-3.43729576	2.071697171
18 H	-2.22190943	-1.98283803	2.10884136
19 H	-0.47048103	-1.82021063	2.280967843
20 C	-3.32019554	-1.28104857	-0.26781234
21 H	-3.72664304	-1.87231212	0.556747718
22 H	-3.94655874	-1.46240459	-1.14411743
23 C	-3.27719926	0.203506639	0.080803644
24 H	-3.21975101	0.849611521	-0.80018635
25 H	-2.43770856	0.440648337	0.749455863
26 N	1.497535991	-0.05185084	0.087585185
27 S	0.695220919	1.180627718	0.720515845
28 O	-0.45022584	0.619842991	1.445504497
29 O	1.486967131	2.231735427	1.352841836
30 C	-0.09912688	2.003297489	-0.75456064
31 F	-0.74637631	1.100181729	-1.49352539
32 F	0.805019103	2.604362151	-1.51254799
33 F	-0.97829435	2.905077858	-0.32521549
34 S	2.997899785	0.026304166	-0.48724858
35 O	3.460398908	1.349539203	-0.89904458
36 O	3.1822952	-1.11415728	-1.38392772
37 C	4.0378407	-0.40185532	1.000934278
38 F	3.689256149	-1.59065685	1.48916701
39 F	5.315639687	-0.44856328	0.636344678
40 F	3.891983216	0.510204985	1.953632194

Table S9. Computationally predicted bond lengths for **3b** at the solvent dielectric constant $\varepsilon_r = 12$ employing the C-PCM treatment.

Bond	Start	End	Order	Length (Å)
Bond 1	H1	C1	1	1.0813
Bond 2	H2	C2	1	1.08108
Bond 3	C1	C2	2	1.35099
Bond 4	C1	N2	1	1.38152
Bond 5	C2	N1	1	1.37645
Bond 6	F3	C8	1	1.32406
Bond 7	F2	C8	1	1.33442
Bond 8	O6	S3	2	1.46242
Bond 9	H10	C6	1	1.09232
Bond 10	O5	S3	2	1.46098
Bond 11	H11	C7	1	1.09404
Bond 12	C8	F4	1	1.33068
Bond 13	C8	S2	1	1.86655
Bond 14	N2	C6	1	1.45578
Bond 15	N2	C3	1	1.34323
Bond 16	H4	C4	1	1.09026
Bond 17	S3	N3	1	1.60866
Bond 18	S3	C9	1	1.86531
Bond 19	N1	C4	1	1.45608
Bond 20	N1	C3	1	1.33268
Bond 21	C6	C7	1	1.52549
Bond 22	C6	H9	1	1.093
Bond 23	F1	S1	1	1.63686
Bond 24	C7	H12	1	1.09909
Bond 25	C7	S1	1	1.77496
Bond 26	N3	S2	1	1.60106
Bond 27	C4	H5	1	1.09411
Bond 28	C4	H3	1	1.0906
Bond 29	C3	C5	1	1.47826
Bond 30	F6	C9	1	1.32961
Bond 31	S2	O4	2	1.45999
Bond 32	S2	O3	2	1.46701
Bond 33	S1	O2	2	1.44427
Bond 34	S1	O1	2	1.44794
Bond 35	C9	F5	1	1.33159
Bond 36	C9	F7	1	1.32694
Bond 37	C5	H6	1	1.09583
Bond 38	C5	H7	1	1.09122
Bond 39	C5	H8	1	1.09435

Table S10. Computationally predicted three-dimensional coordinates for **3b** at the solvent dielectric constant $\epsilon_r = 12$ employing the C-PCM treatment.

Atom	Coordinates (Å)		
	X	Y	Z
1 S	-4.71237026	0.724695471	0.979623
2 F	-5.84501753	0.408826026	-0.15908
3 O	-5.00754062	-0.1784646	2.072194
4 O	-4.71805735	2.158407057	1.153832
5 N	-0.00827266	-2.61832261	-0.37042
6 N	-1.98192701	-1.77886252	-0.57421
7 C	-1.43110014	-1.82714483	-1.84025
8 H	-1.9697746	-1.47365025	-2.70863
9 C	-0.19315518	-2.3517285	-1.70809
10 H	0.579851646	-2.54638666	-2.43836
11 C	-1.0935218	-2.25615925	0.313026
12 C	1.186982093	-3.21081786	0.213082
13 H	1.423520929	-2.69401284	1.143867
14 H	2.009543299	-3.06441395	-0.48736
15 H	1.018598234	-4.27603314	0.397553
16 C	-1.25748395	-2.38746566	1.776287
17 H	-1.20697673	-3.44286887	2.066831
18 H	-2.21055212	-1.97383264	2.109956
19 H	-0.45674336	-1.83743156	2.280147
20 C	-3.31771479	-1.28739056	-0.26854
21 H	-3.72172889	-1.87788569	0.557741
22 H	-3.94457574	-1.47217368	-1.14379
23 C	-3.27767053	0.197888389	0.077084
24 H	-3.21958764	0.842294387	-0.80512
25 H	-2.439732	0.437011411	0.746927
26 N	1.494516299	-0.04780662	0.092443
27 S	0.689449471	1.182835289	0.725508
28 O	-0.45565195	0.61971969	1.449224
29 O	1.478877732	2.234831864	1.359279
30 C	-0.10547181	2.005439766	-0.74943
31 F	-0.74508136	1.100774288	-1.49318
32 F	0.797004898	2.614704865	-1.50274
33 F	-0.99151635	2.900332764	-0.31954
34 S	2.994606032	0.03442414	-0.48268
35 O	3.453658767	1.359212217	-0.89339
36 O	3.181841037	-1.10475065	-1.3804
37 C	4.035511384	-0.3925737	1.005132
38 F	3.689242541	-1.58235506	1.492638
39 F	5.313363107	-0.43660993	0.640408
40 F	3.88795692	0.518653988	1.958376

Table S11. Computationally predicted three-dimensional coordinates for **3b** at the solvent dielectric constant $\epsilon_r = 24$ employing the C-PCM treatment.

Bond	Start	End	Order	Length (Å)
Bond 1	H1	C1	1	1.08159
Bond 2	H2	C2	1	1.08136
Bond 3	C1	C2	2	1.35096
Bond 4	C1	N2	1	1.38153
Bond 5	C2	N1	1	1.37725
Bond 6	F3	C8	1	1.32617
Bond 7	F2	C8	1	1.33161
Bond 8	O6	S3	2	1.46186
Bond 9	H10	C6	1	1.0925
Bond 10	H11	C7	1	1.09447
Bond 11	C8	F4	1	1.33038
Bond 12	C8	S2	1	1.86505
Bond 13	O5	S3	2	1.46259
Bond 14	H4	C4	1	1.09023
Bond 15	N2	C6	1	1.45566
Bond 16	N2	C3	1	1.34324
Bond 17	S3	N3	1	1.60689
Bond 18	S3	C9	1	1.86439
Bond 19	N1	C4	1	1.45626
Bond 20	N1	C3	1	1.33322
Bond 21	F1	S1	1	1.6355
Bond 22	C6	C7	1	1.52436
Bond 23	C6	H9	1	1.09247
Bond 24	C7	H12	1	1.09866
Bond 25	C7	S1	1	1.77419
Bond 26	C4	H5	1	1.09401
Bond 27	C4	H3	1	1.09029
Bond 28	N3	S2	1	1.60149
Bond 29	C3	C5	1	1.478
Bond 30	S2	O4	2	1.46171
Bond 31	S2	O3	2	1.46528
Bond 32	F6	C9	1	1.32997
Bond 33	S1	O2	2	1.44576
Bond 34	S1	O1	2	1.44808
Bond 35	C9	F5	1	1.32991
Bond 36	C9	F7	1	1.32809
Bond 37	C5	H6	1	1.09606
Bond 38	C5	H7	1	1.09101
Bond 39	C5	H8	1	1.09376

Table S12. Computationally predicted three-dimensional coordinates for **3b** at the solvent dielectric constant $\epsilon_r = 24$ employing the C-PCM treatment.

Atom	Coordinates (Å)		
	X	Y	Z
1 S	-4.75095197	0.801424745	0.89460171
2 F	-5.84247907	0.487048106	-0.28208115
3 O	-5.14650817	-0.02843963	2.013435152
4 O	-4.69802079	2.242156269	1.002809732
5 N	-0.03420504	-2.61829752	-0.41937287
6 N	-2.03276801	-1.82038483	-0.51837636
7 C	-1.55384186	-1.86888751	-1.81332505
8 H	-2.15072925	-1.53656233	-2.65185382
9 C	-0.30039156	-2.36848252	-1.74736223
10 H	0.431183523	-2.56391199	-2.51933151
11 C	-1.08739831	-2.27309992	0.321633802
12 C	1.198297071	-3.19864854	0.095225368
13 H	1.461871182	-2.70668387	1.031832977
14 H	1.987540349	-3.01245638	-0.63348558
15 H	1.061880627	-4.27269519	0.252314891
16 C	-1.17325394	-2.40965402	1.790802895
17 H	-1.15362366	-3.46975111	2.068589252
18 H	-2.0876314	-1.95799756	2.178379071
19 H	-0.32165287	-1.90285124	2.253650704
20 C	-3.35234581	-1.33086321	-0.14684591
21 H	-3.68683415	-1.86640398	0.744669655
22 H	-4.0369847	-1.57770871	-0.961638
23 C	-3.29772763	0.173416282	0.093664545
24 H	-3.19643203	0.748723697	-0.83187954
25 H	-2.47979103	0.445398909	0.774879414
26 N	1.5479596	-0.02822252	0.096659257
27 S	0.698160184	1.180490891	0.714415946
28 O	-0.44014523	0.596739444	1.42915153
29 O	1.451035845	2.259083391	1.351932118
30 C	-0.0861713	1.968589899	-0.78295915
31 F	-0.72817686	1.051746458	-1.50436333
32 F	0.830105636	2.548881799	-1.54612616
33 F	-0.96224047	2.885746302	-0.38141445
34 S	3.065074011	0.086497508	-0.42036426
35 O	3.530135609	1.429381366	-0.76612851
36 O	3.302364953	-1.01408082	-1.35281647
37 C	4.052916438	-0.37912767	1.09069803
38 F	3.738843103	-1.60630561	1.495728334
39 F	5.347695993	-0.34589114	0.788601675
40 F	3.818491003	0.473022733	2.082018292

7. Prediction of dielectric constants

Method Validation. As explained in the main article, some technical details of our approach were modified compared to the approach proposed by Krossing and co-workers. We therefore scaled the computational descriptors to match the published values.⁹

Specifically, we observed that the ratio between the molecular volumes (V_m) determined in this work and the published results is close to constant (Table S13). We therefore applied the average ratio as a uniform scaling factor to reproduce the published molecular volumes.

Table S13. Comparison of molecular volumes determined in this work as compared to the published results,⁹ the ratio between unscaled volumes from this work and published results, and the molecular volumes scaled by the average ratio. The average deviation and root mean square deviation between scaled volumes from this work and published results is reported in the bottom two rows, respectively.

IL	This work	Krossing et al. ⁹	Ratio	This work
	Unscaled (nm ³)	(nm ³)		Scaled (nm ³)
[C ₄ mIm][BF ₄]	0.192	0.279	1.458	0.280
[C ₆ mIm][BF ₄]	0.223	0.318	1.428	0.325
[C ₆ mIm][PF ₆]	0.242	0.349	1.444	0.352
[C ₈ mIm][BF ₄]	0.253	0.377	1.490	0.369
[C ₈ mIm][PF ₆]	0.273	0.403	1.476	0.399
Average			1.459	0.000
RMSD				0.006

Moreover, differences in the solvent approach and the calculation of isolated cations and anions (Ref. 9) versus combined cation/anion pairs (this work) led to differences in the predicted absolute magnitudes of the solvation free energies (Table S14). We again observed a fairly constant ratio between the solvation energies reported in this work and the energies reported by the Krossing group. We therefore applied the average ratio as a uniform scaling factor and obtained a good agreement within the training set with average error of 0.05 kJ/mol and root mean square deviation of 2.66 kJ/mol (Table S2). For an independent validation and to test the transferability of the scaling to other systems, we chose a different test set of ILs (Table S15). The agreement between the scaled solvation energies from this work and the previously published results is again good, although errors are somewhat larger with an average of 0.645 kJ/mol and root mean squared deviation of 8.245 kJ/mol (Table S15).

Table S14. Solvation free energies obtained in this work as compared to energies reported by Krossing and co-workers. The average ratio was applied to scale our results, which results in good agreement with the values reported previously.⁹

IL	This work	Previous work ⁹	Ratio	This work
	Unscaled (kJ/mol)	(kJ/mol)		Scaled (kJ/mol)
[C ₄ mIm][BF ₄]	-222	-473	2.129	-471
[C ₄ mIm][PF ₆]	-212	-446	2.105	-449
[C ₂ mIm][BF ₄]	-224	-475	2.123	-474
Average			2.119	0.050
RMSD				2.66

Table S15. Validation of the scaling factors for the solvation free energies.

IL	Previous work ⁹ (kJ/mol)	This work Scaled (kJ/mol)
[C ₆ mIm][BF ₄]	-473	-475
[C ₈ mIm][BF ₄]	-473	-462
[C ₆ mIm][PF ₆]	-446	-445
[C ₈ mIm][PF ₆]	-447	-455
Average Error:		0.645
RMSD		8.245

To assess the accuracy of the approach for predicting dielectric constants, we selected a set of ILs comprising both the training systems discussed above as well as three independent test systems (Table S16). Our approach reproduces the published dielectric constants to with an average error of -0.1 and a root mean square deviation of 1.3, which is an excellent fidelity relative to the published computational results.

Table S16. Validation of dielectric constant prediction.

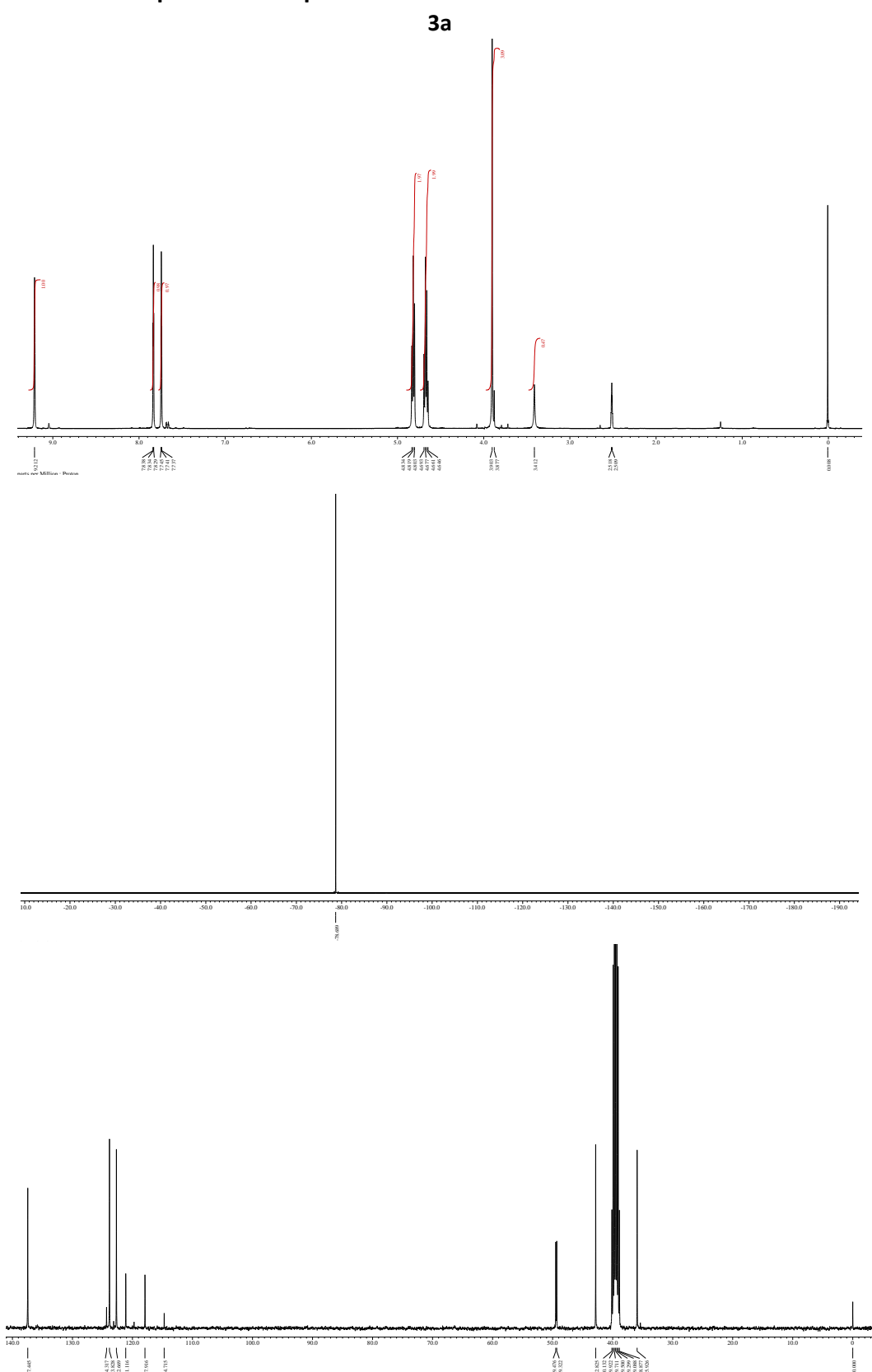
IL	Previous work ⁹	This work
[C ₄ mIm][BF ₄]	14	13.6
[C ₆ mIm][BF ₄]	16	16.8
[C ₈ mIm][BF ₄]	19	16.2
[C ₄ mIm][PF ₆]	10	10.5
[C ₆ mIm][PF ₆]	12	11.9
[C ₈ mIm][PF ₆]	15	16.5
[C ₂ mIm][BF ₄]	12	11.9
Average Error:		-0.1
RMSD		1.3

Utilizing the approach as outlined above, we obtain $V_m = 0.459 \text{ nm}^3$ and $\Delta G_s = -490.453 \text{ kJ/mol}$ for **3b**. Inserting into the equation for the dielectric constant, we obtain $\varepsilon_r = 26.8$.

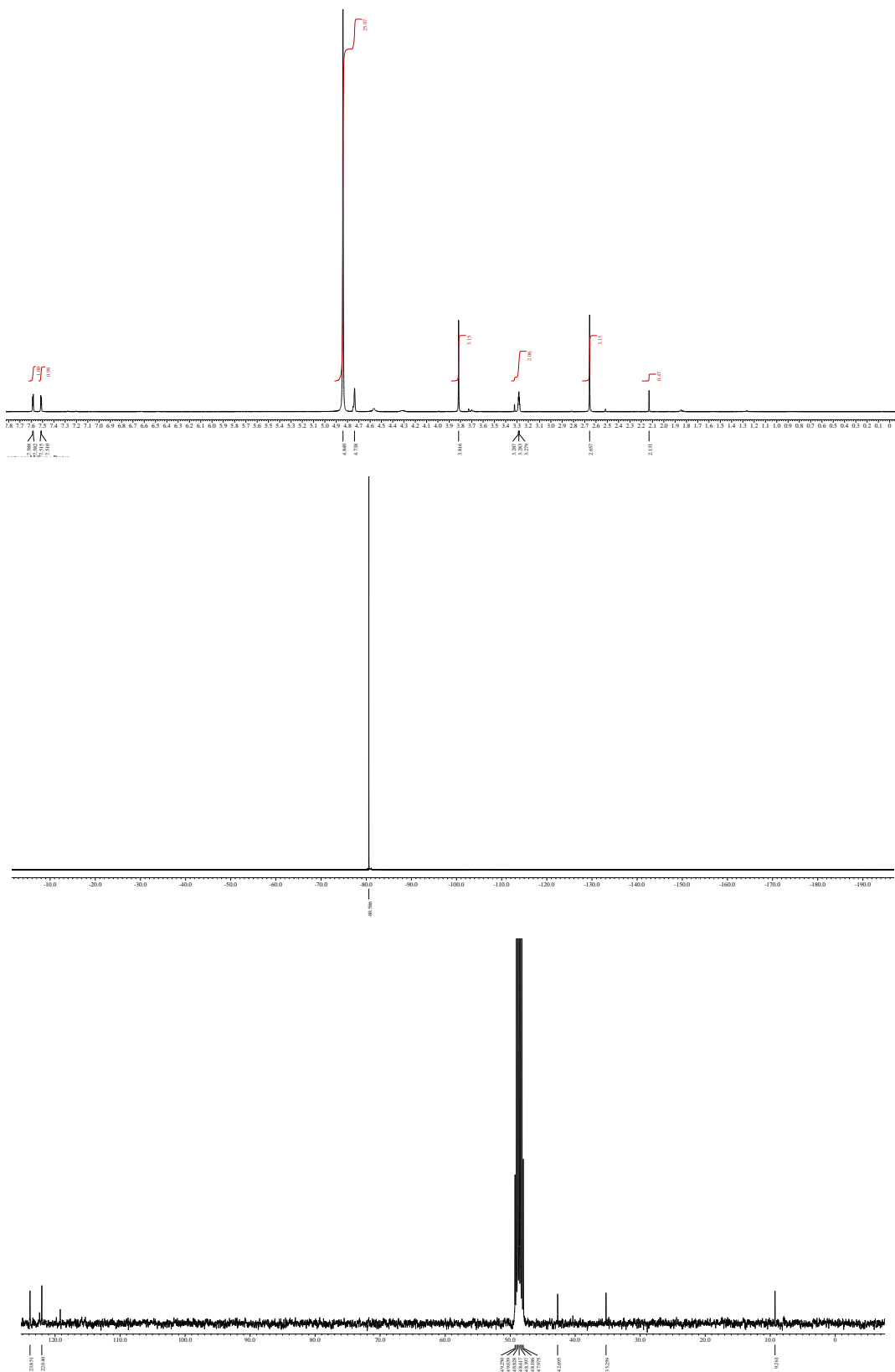
References

1. L. Krause, R. Herbst-Irmer, G. M. Sheldrick and D. Stalke, Comparison of silver and molybdenum microfocus X-ray sources for single-crystal structure determination. *J. Appl. Cryst.*, 2015, **48**, 3–10.
2. Q. Zheng, J. Dong and K. B. Sharpless, Ethenesulfonyl fluoride (ESF): an on-water procedure for the kilogram-scale preparation. *J. Org. Chem.*, 2016, **81**, 11360–11362.
3. Bruker, Apex3 v2019.1-0, SAINT V8.40A, 2019, Bruker AXS Inc., Madison, Wisconsin, USA
4. a) SHELXTL suite of programs, Version 6.14, 2000–2003, Bruker Advanced X-ray Solutions, Bruker AXS Inc., Madison, Wisconsin, USA b) G. M. Sheldrick, A short history of SHELX. *Acta Crystallogr. A.*, 2008, **64**, 112–122.
5. a) G. M. Sheldrick, University of Göttingen, Germany, 2018. b) G. M. Sheldrick, Crystal structure refinement with SHELXL. *Acta Crystallogr. Sect. C, Struct. Chem.*, 2015, **71**, 3–8.
6. C. B. Hübschle, G. M. Sheldrick and B. Dittrich, ShelXle: a Qt graphical user interface for SHELXL. *J. Appl. Crystallogr.*, 2011, **44**, 1281–1284.
7. O. V. Dolomanov, L.J., Bourhis, R. J., Gildea, J. A. K. , Howard, and H. J. Puschmann, OLEX2: a complete structure solution, refinement and analysis program. *J. Appl. Cryst.*, 2009, **42**, 339–341.
8. G. M. Sheldrick, *TWINABS* 2012/1. 2012, Bruker, Madison, Wisconsin, USA.
9. P. Eiden, S. Bulut, T. Köchner, C. Friedrich, T. Schubert and I. Krossing, *J. Phys. Chem. B.*, 2011, **115**, 300–309.

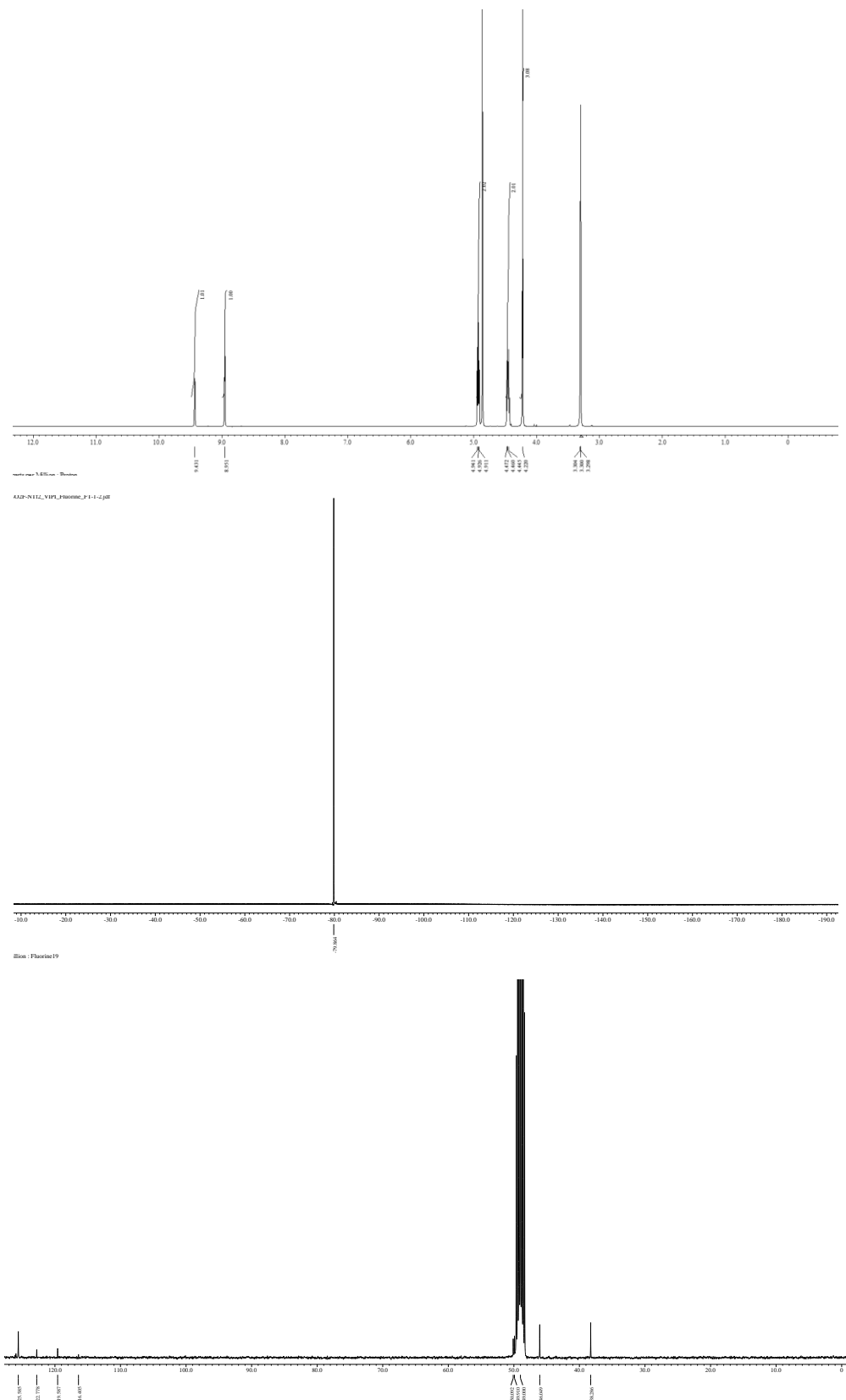
¹H, ¹⁹F and ¹³C NMR spectra of the products



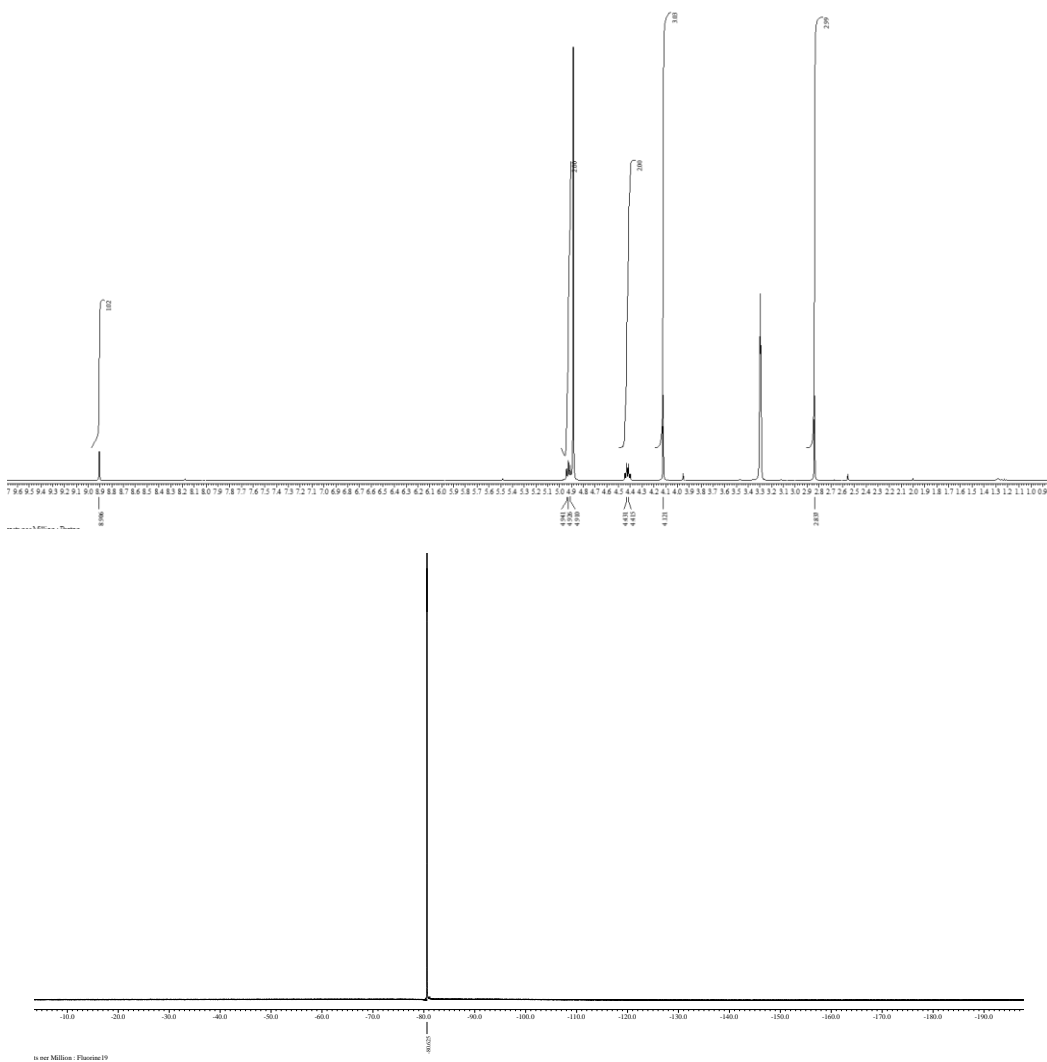
3b



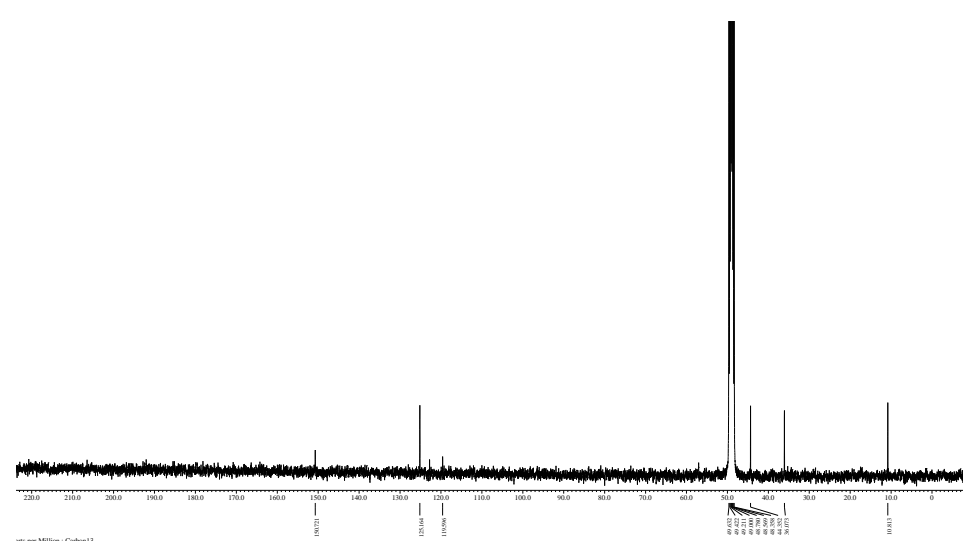
3c



3d

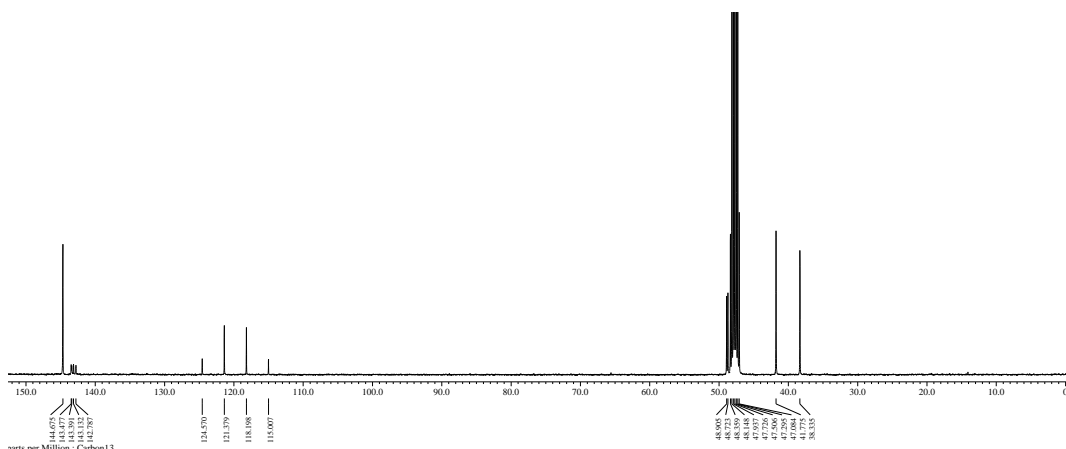
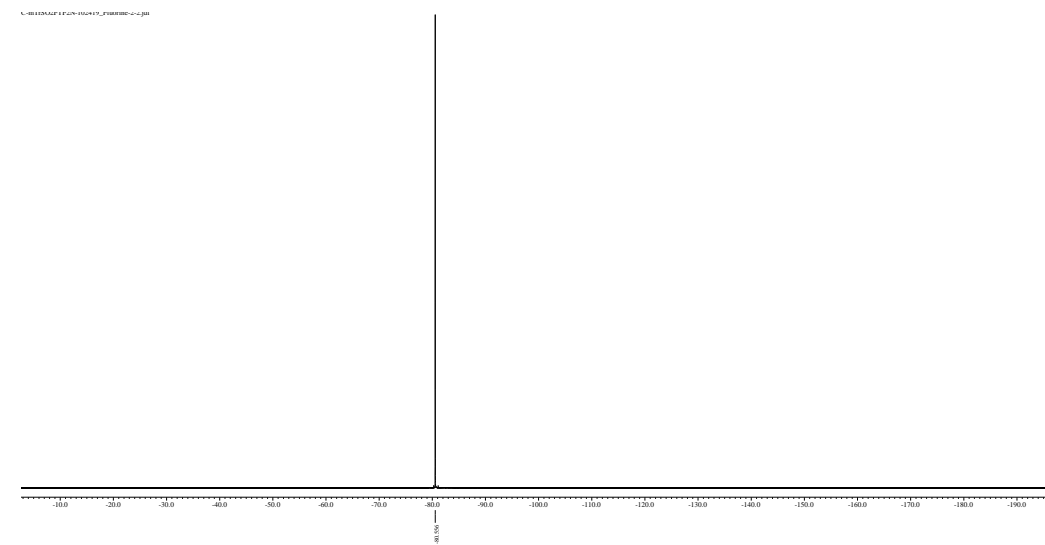
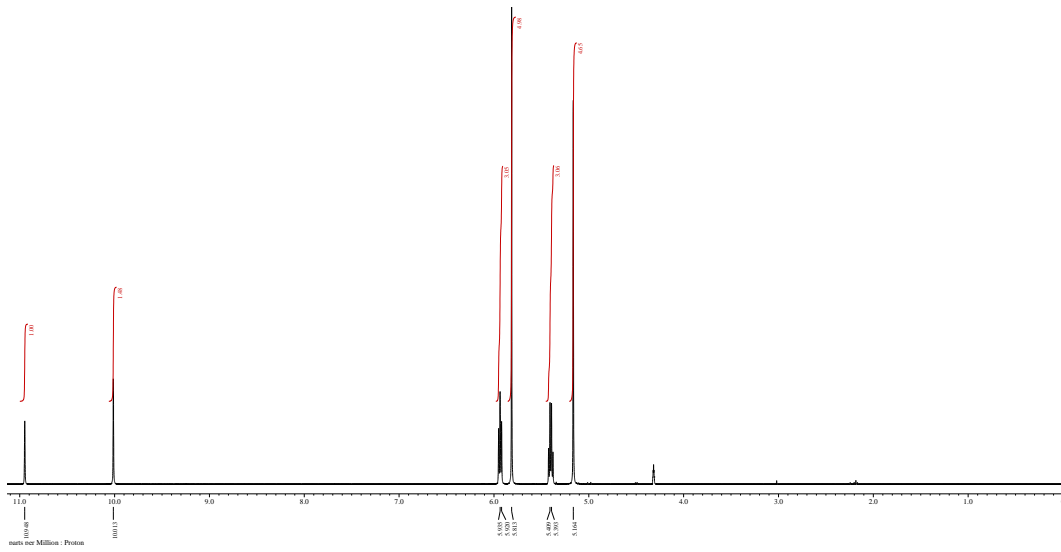


int over Million : Fluorescein

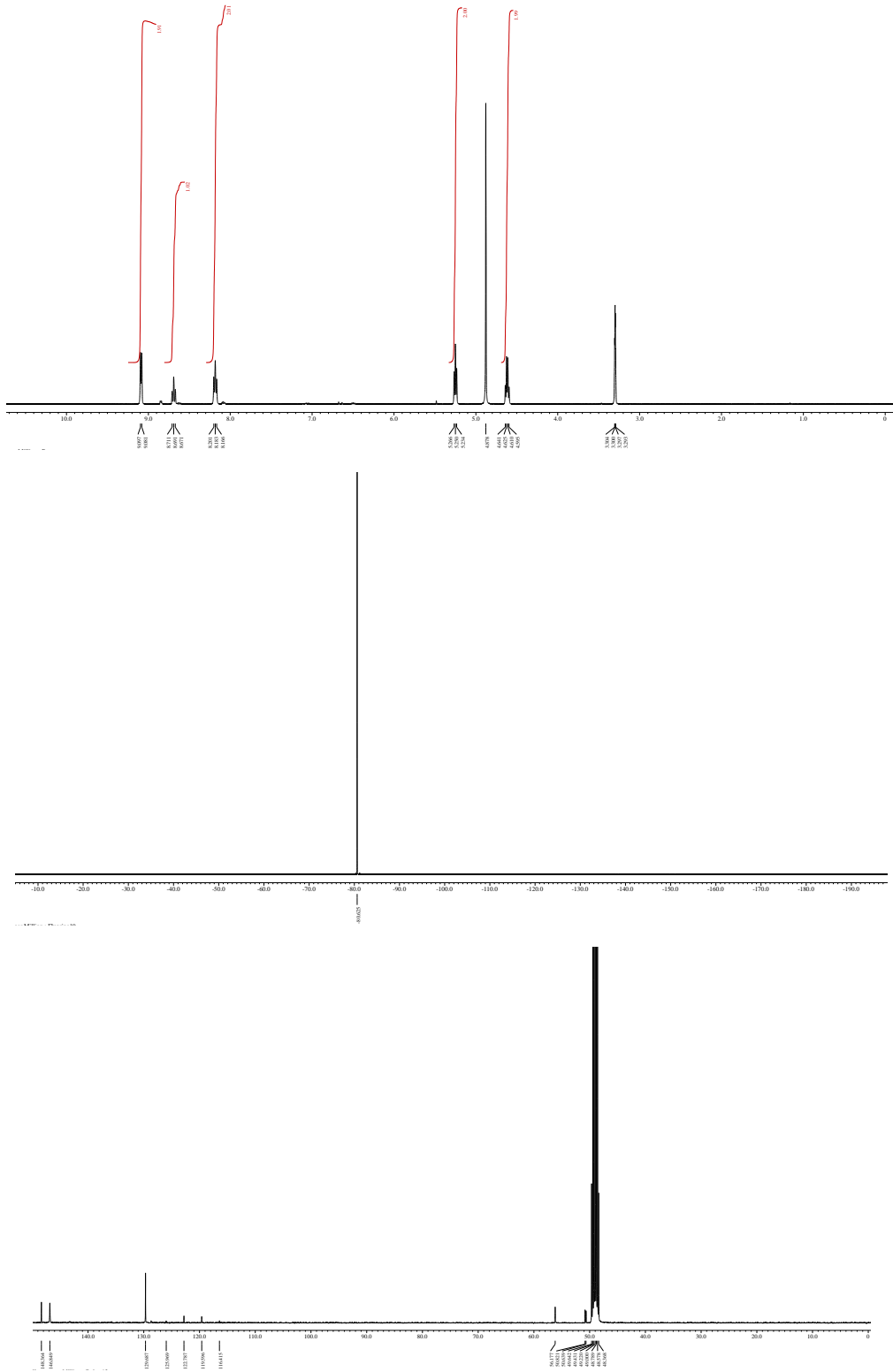


int over Million : Curvlett

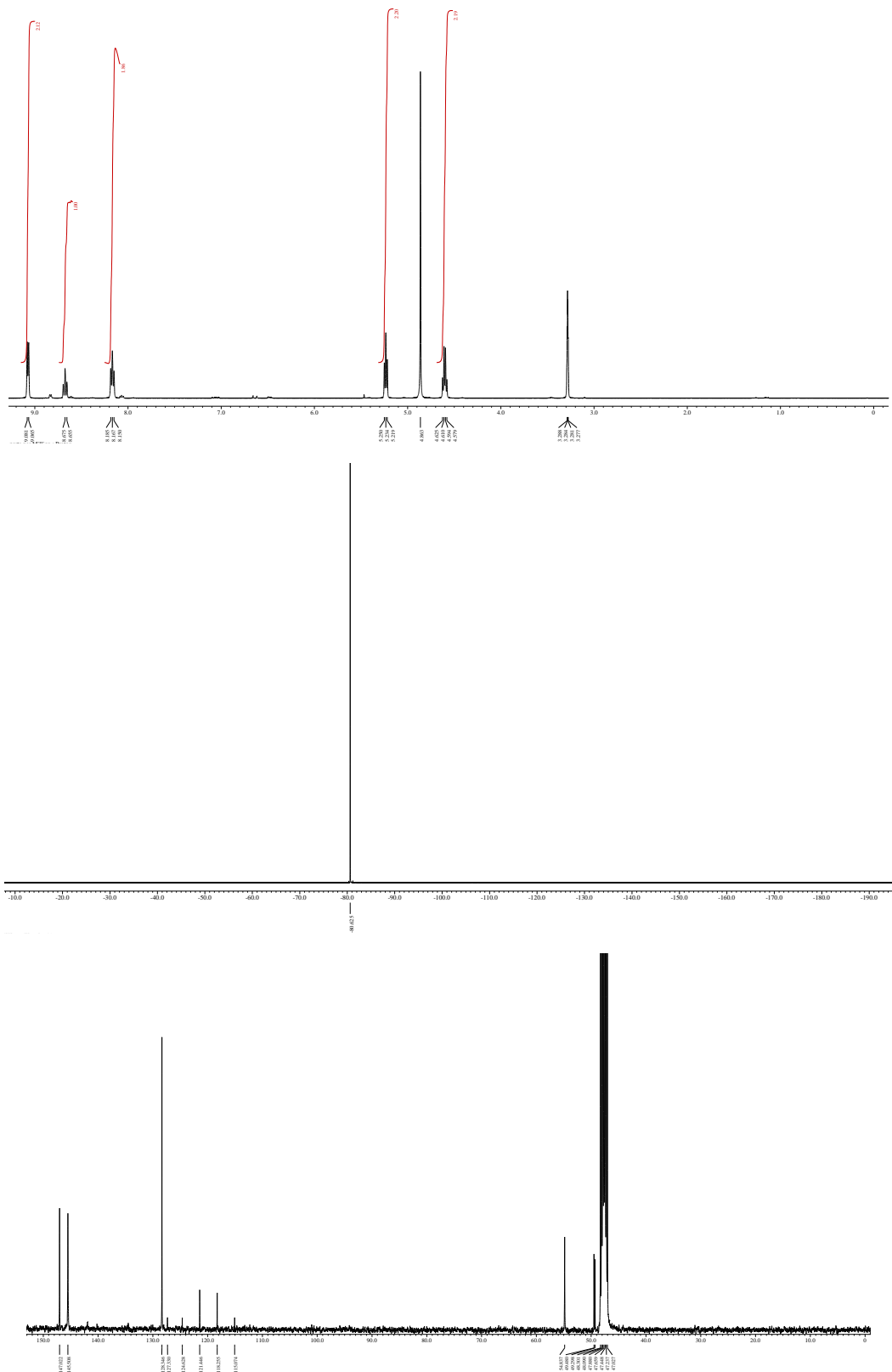
3e

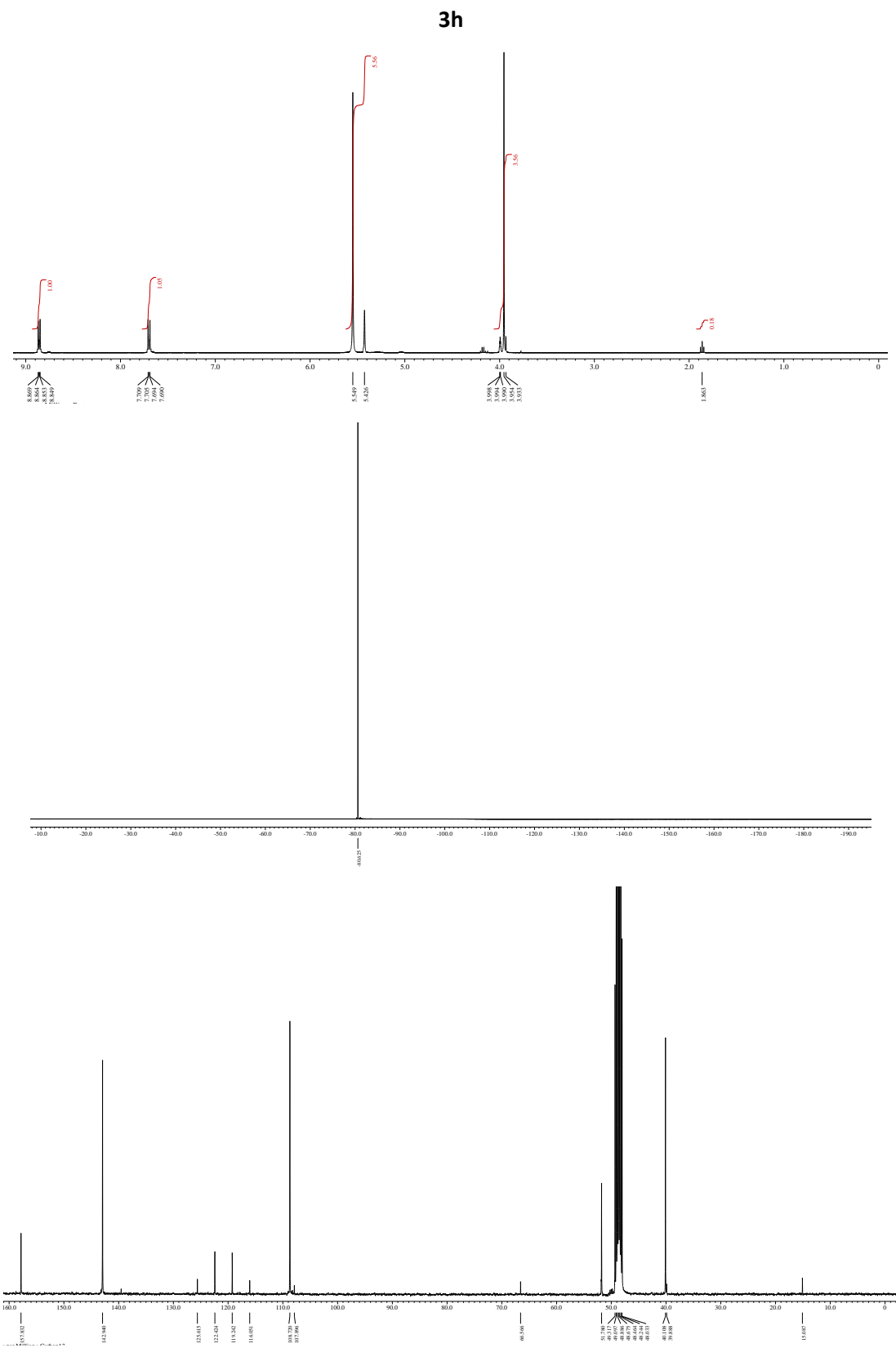


3f

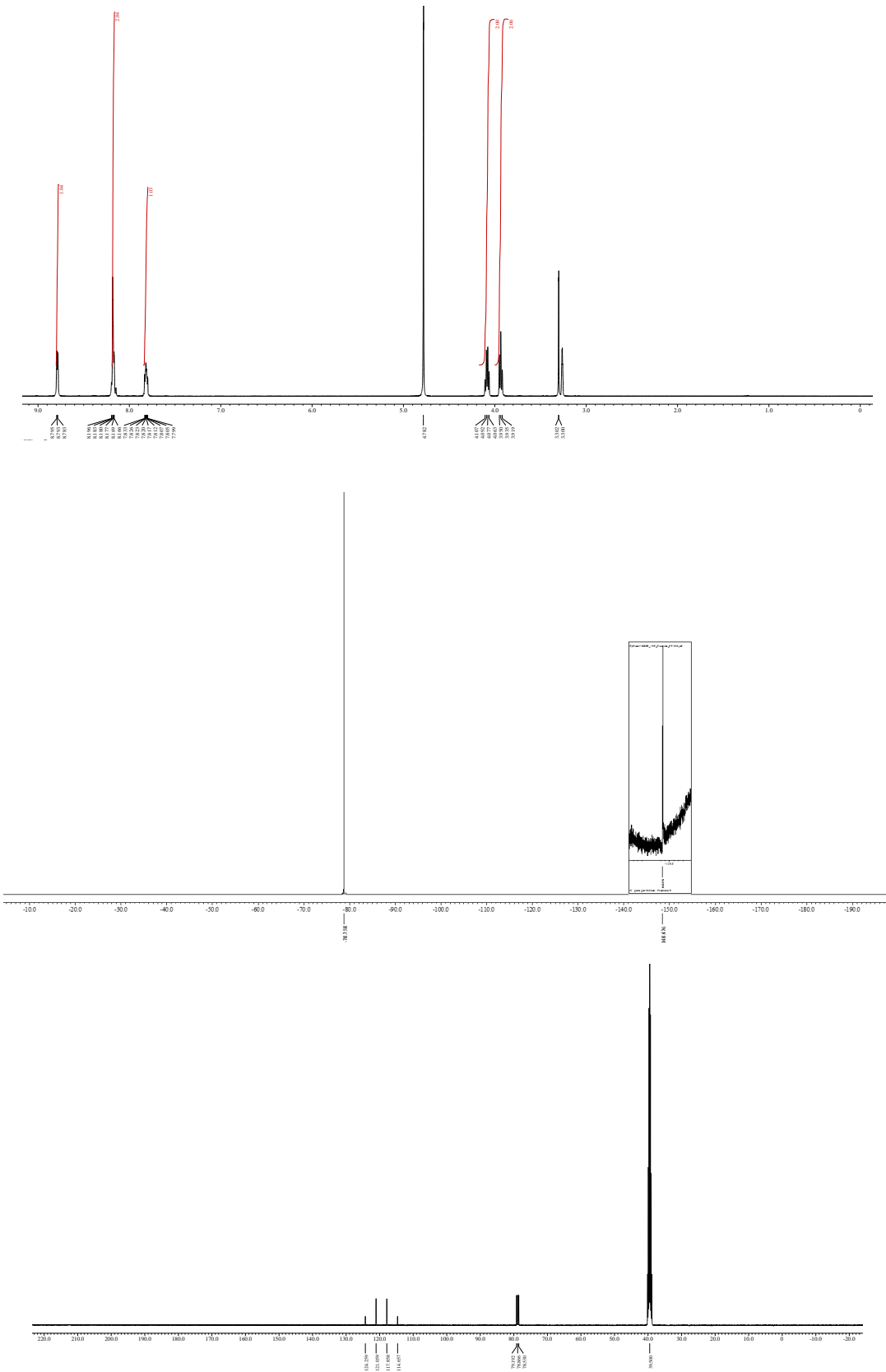


3g

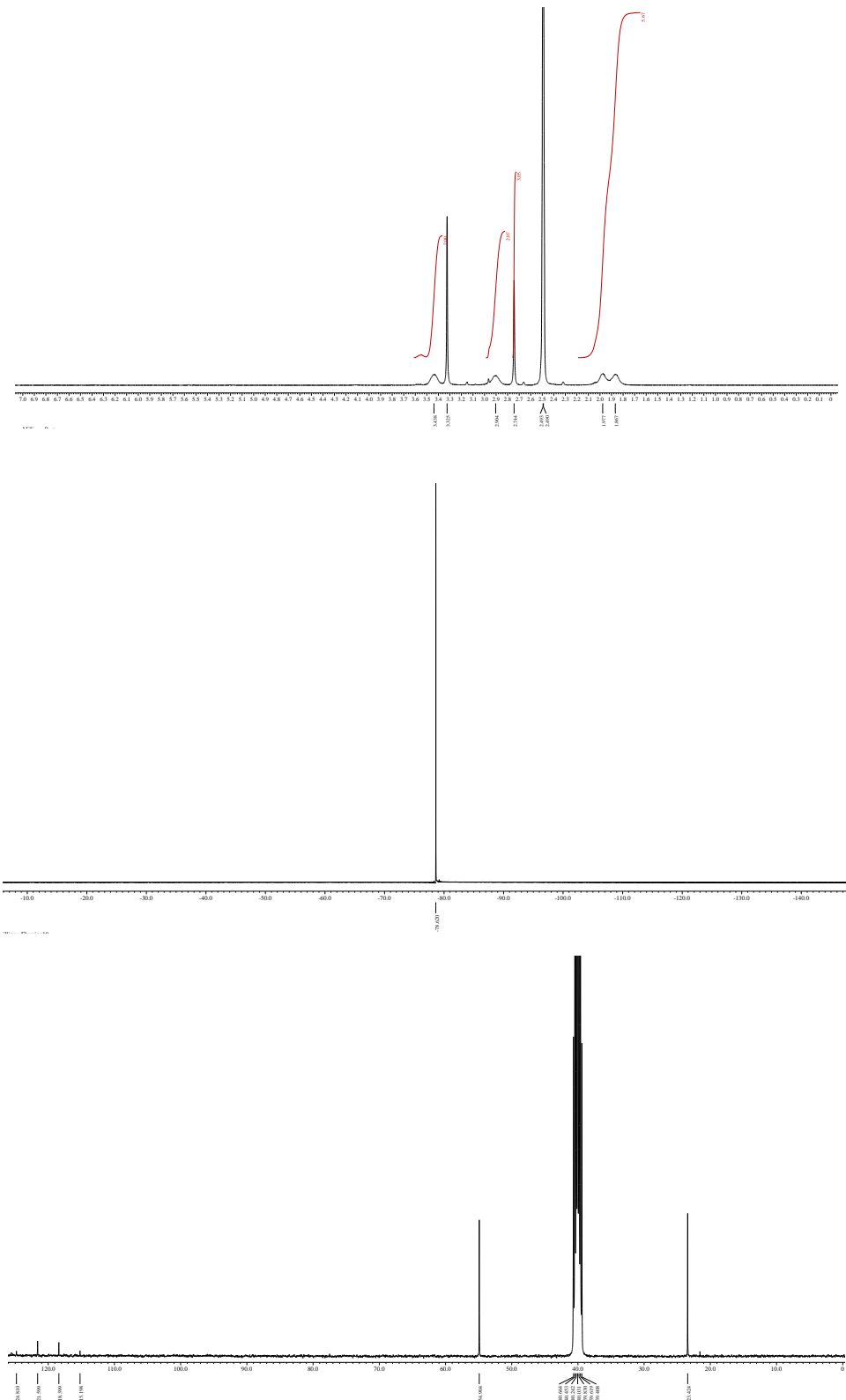


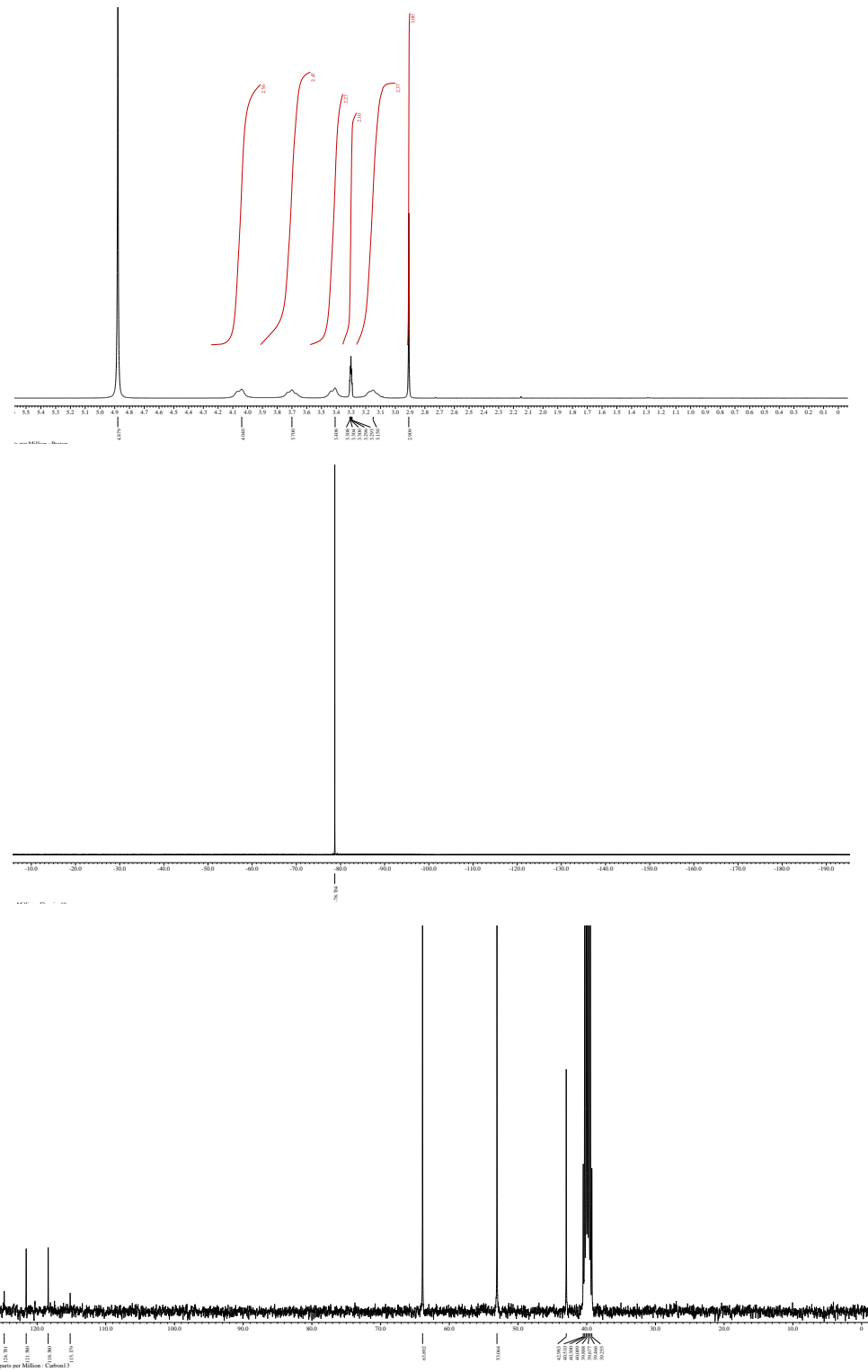


3i

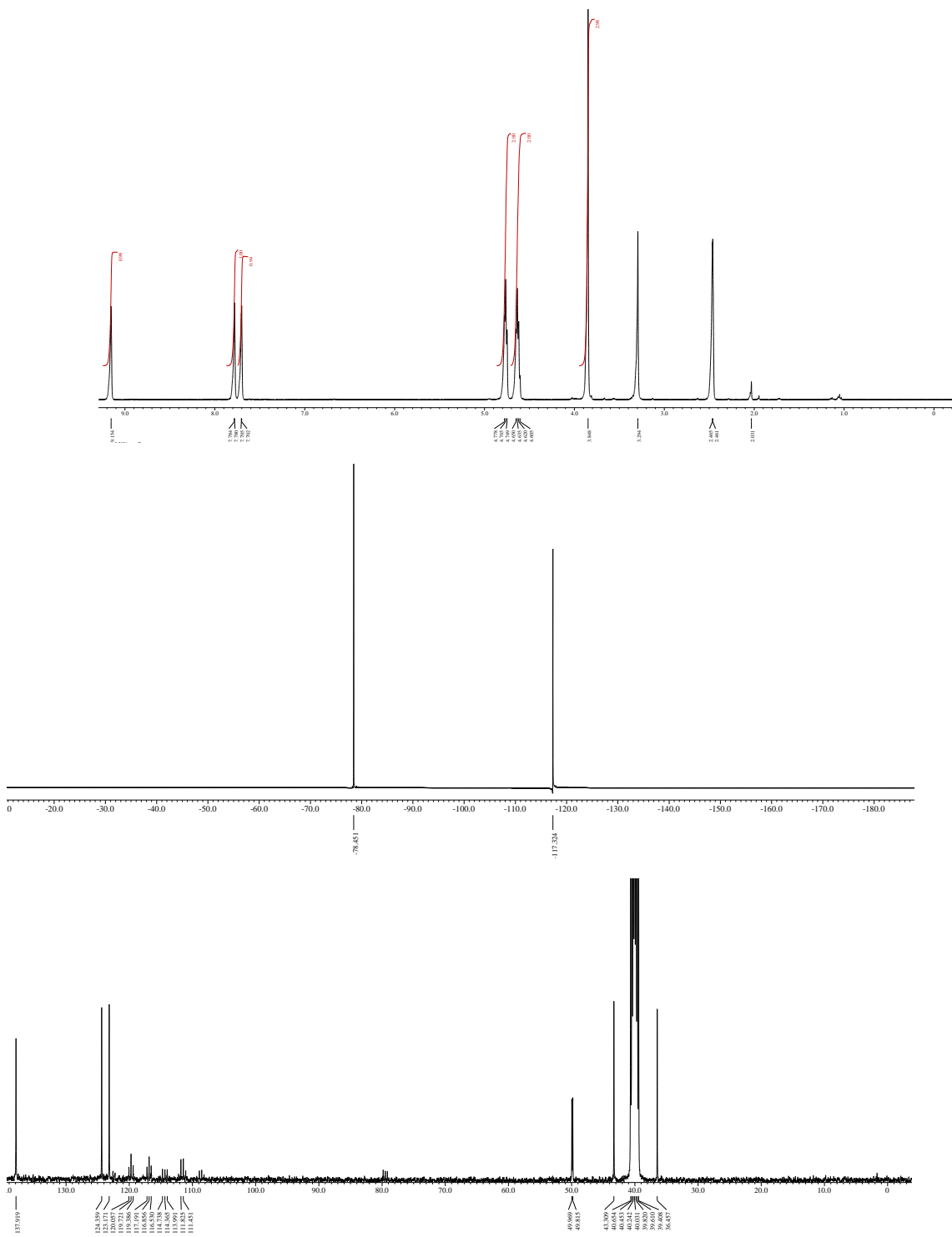


3j

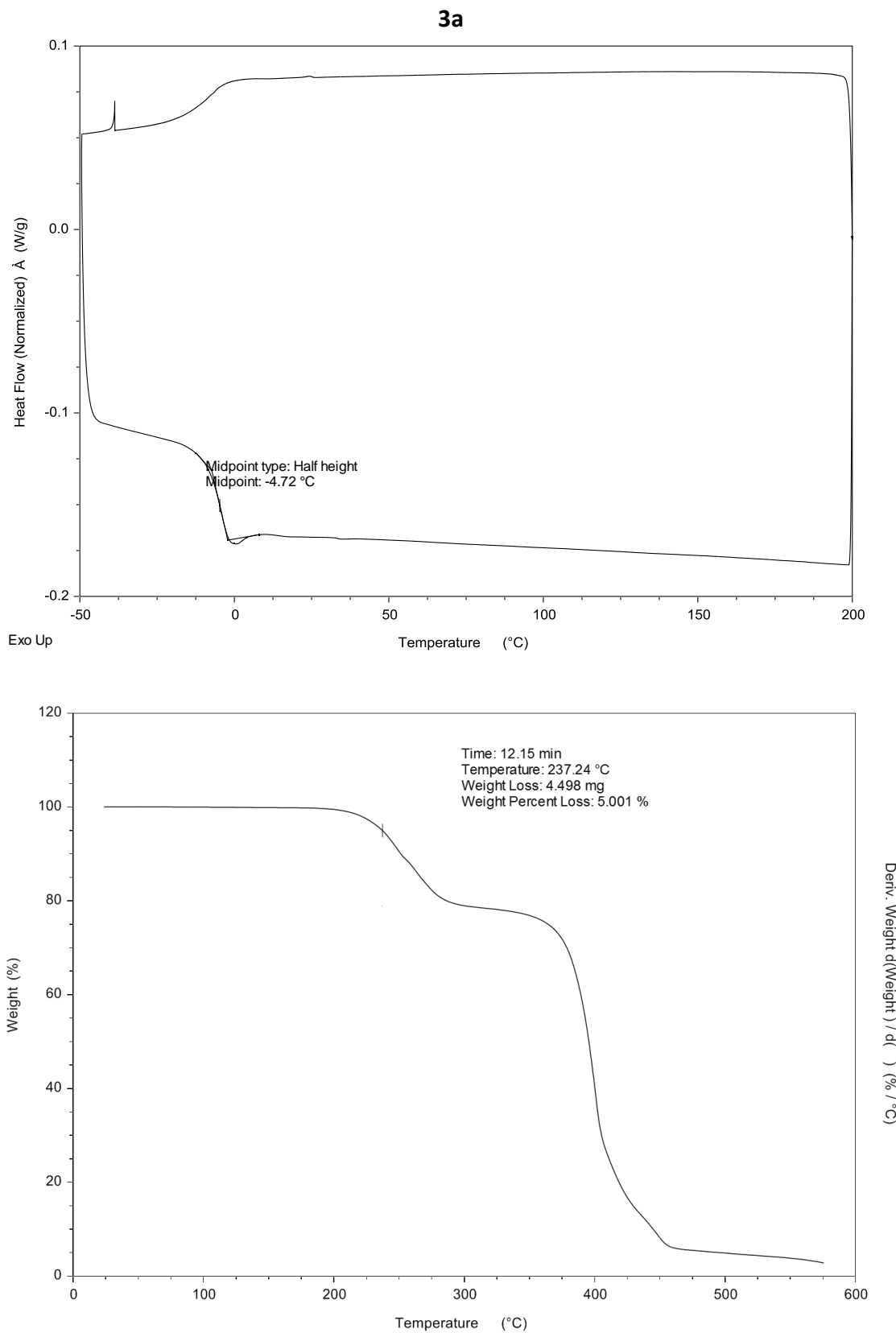




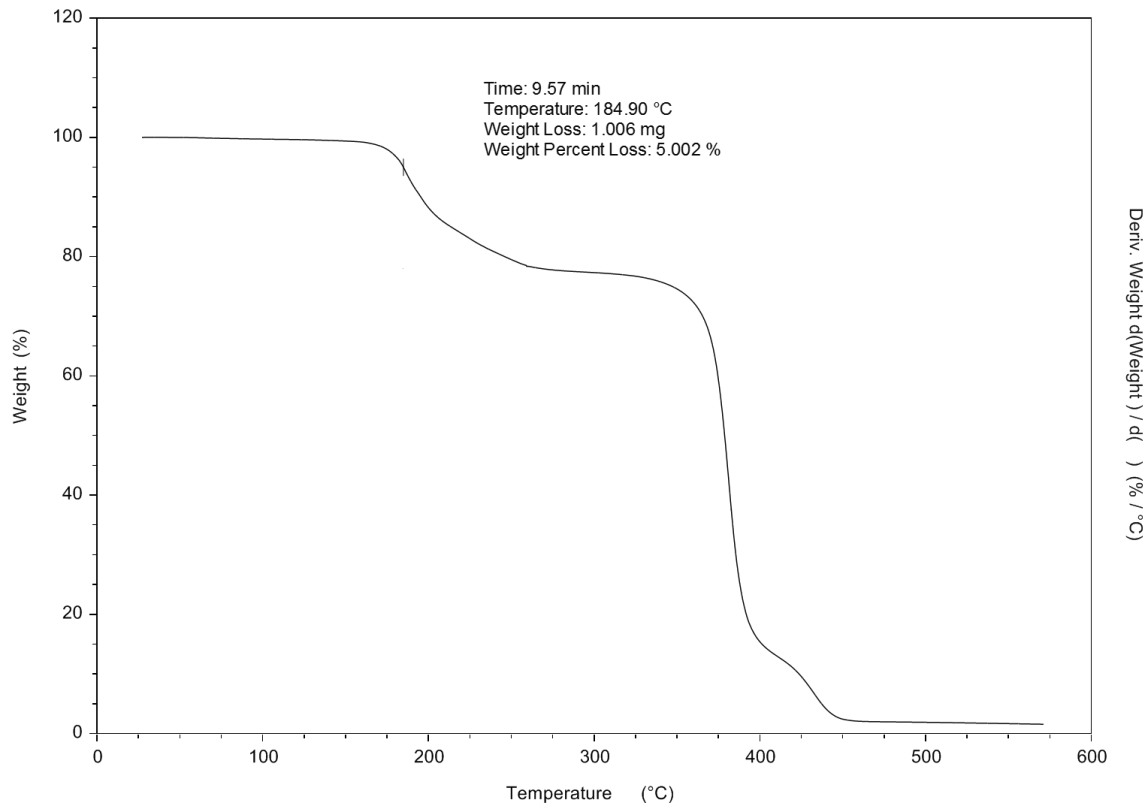
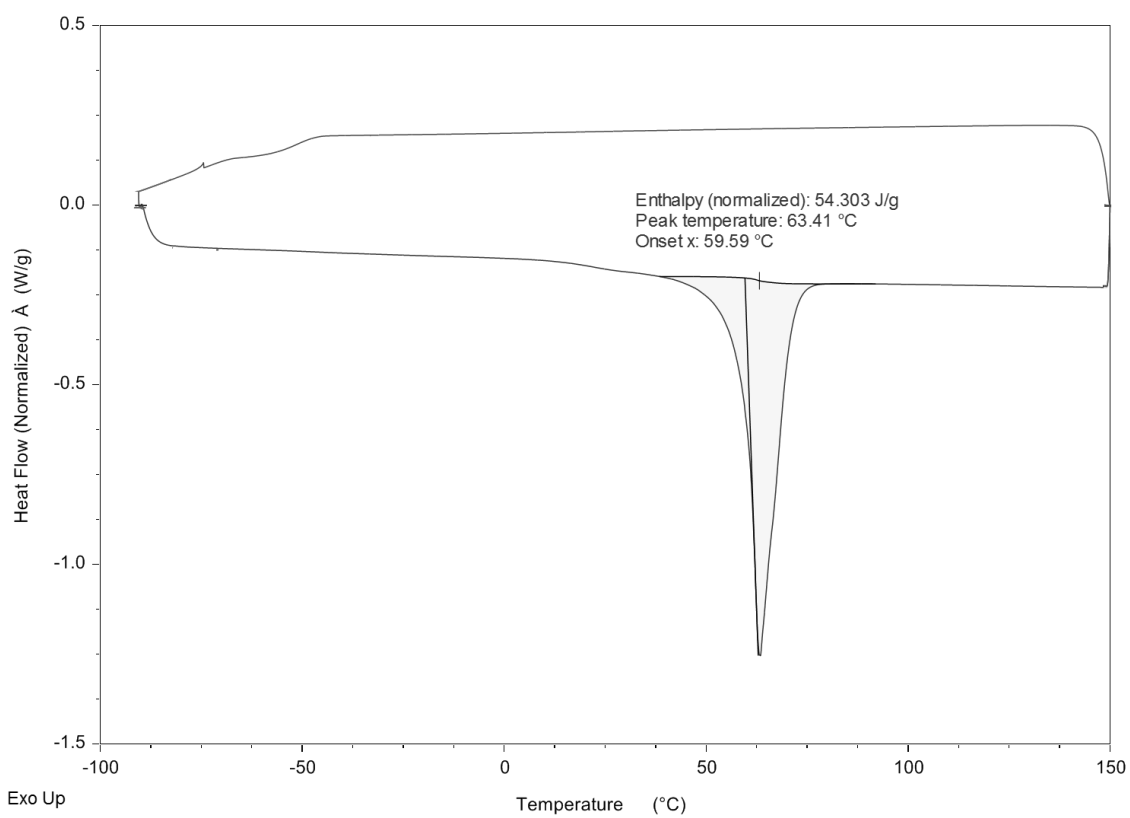
3a-BETI



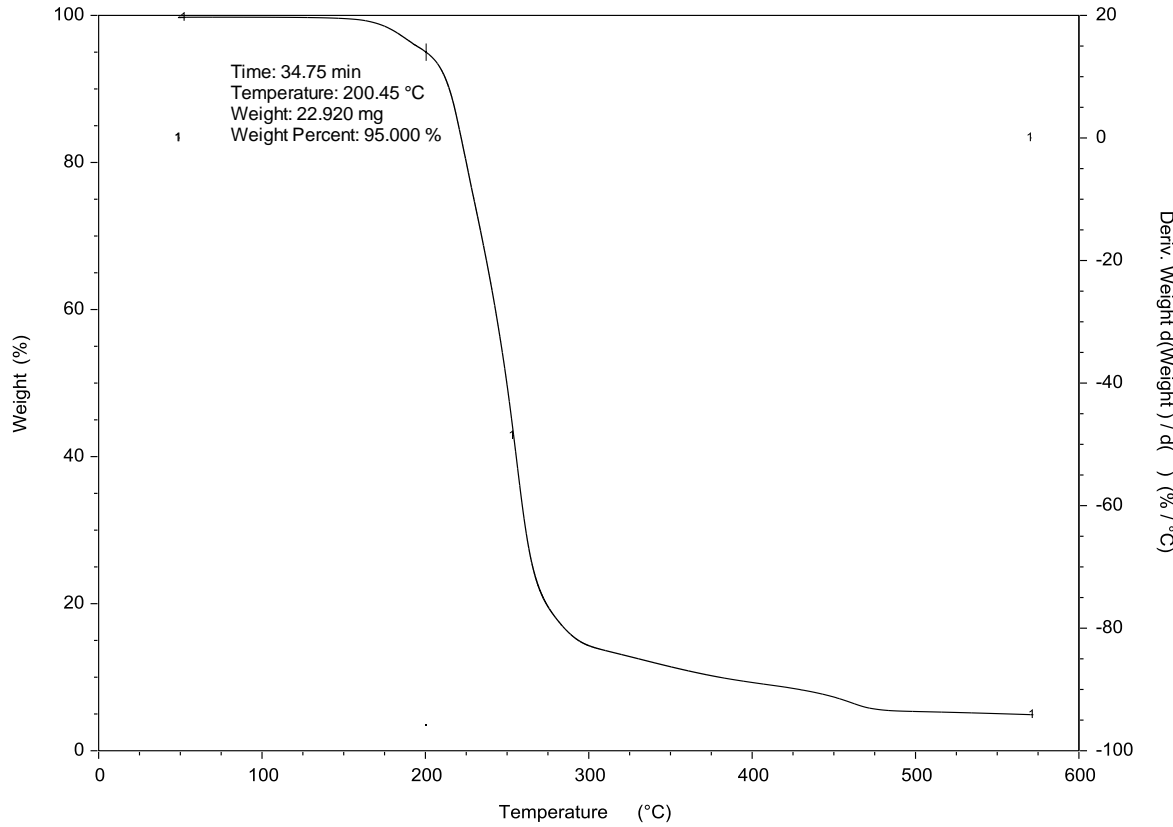
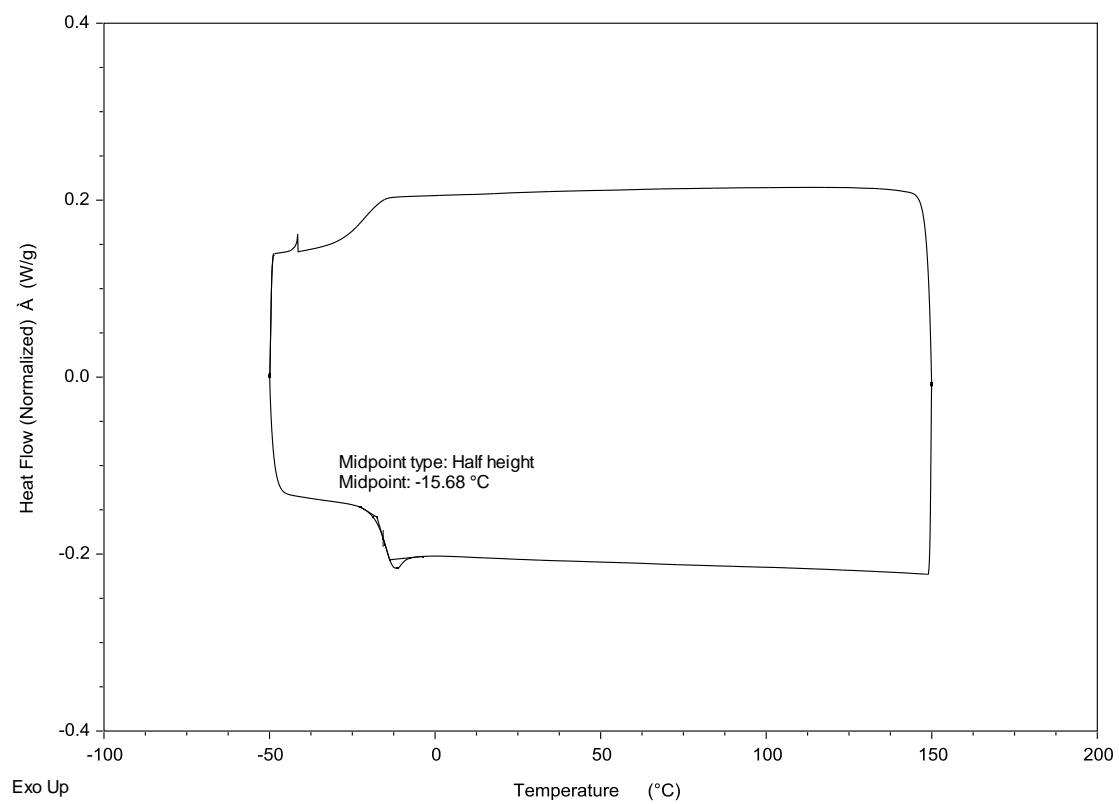
DSC and TGA thermograms of the products



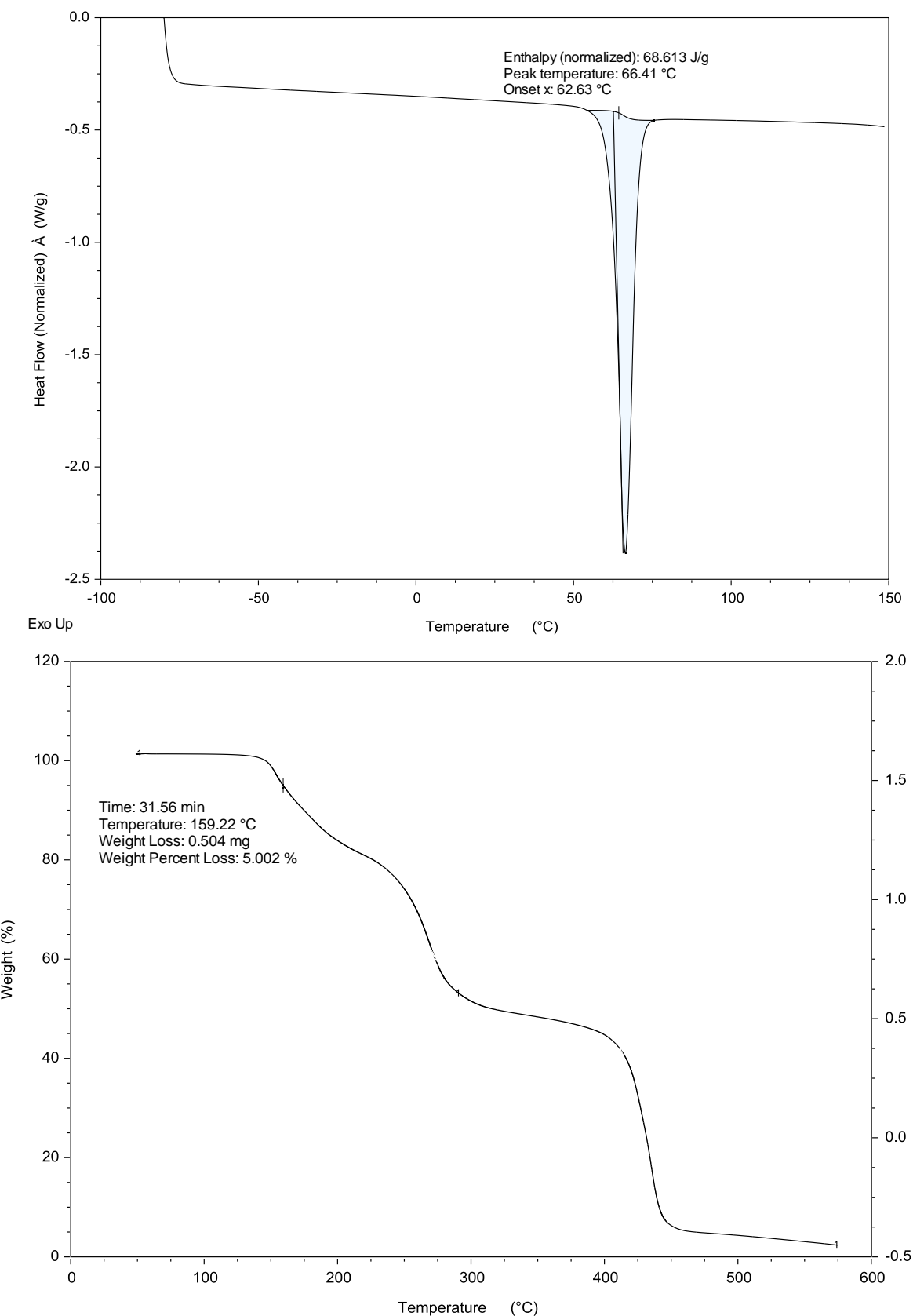
3b



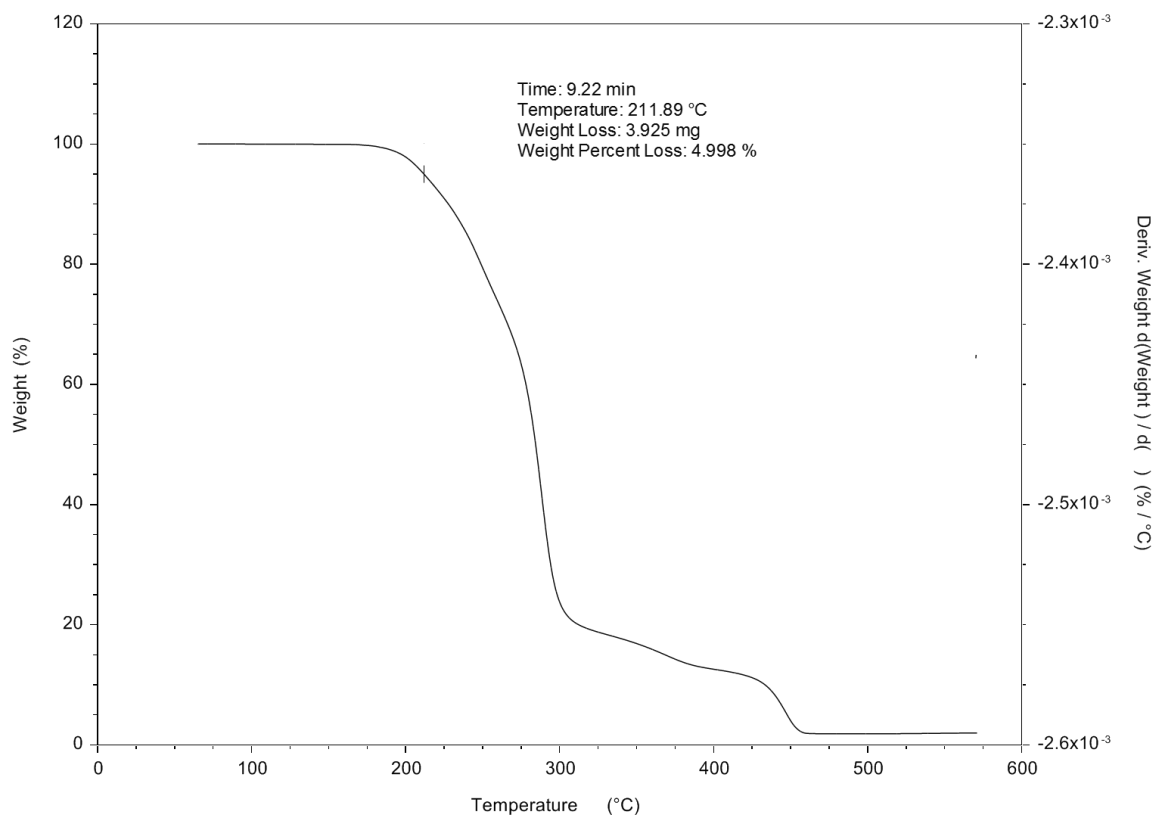
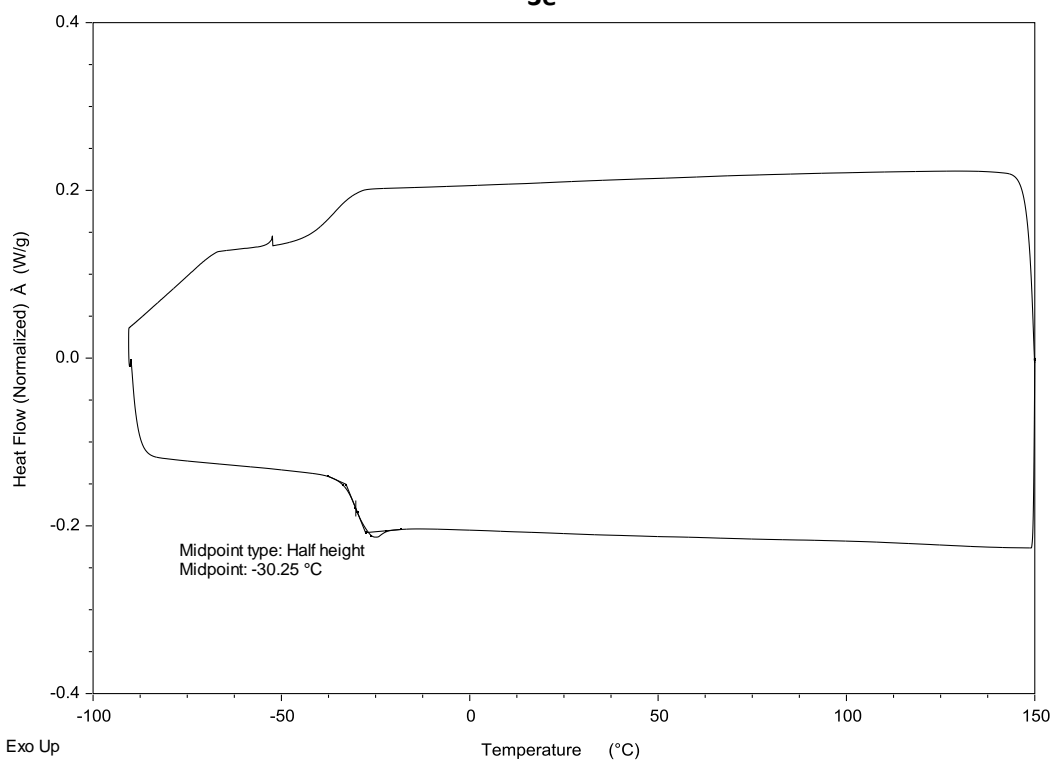
3c



3d

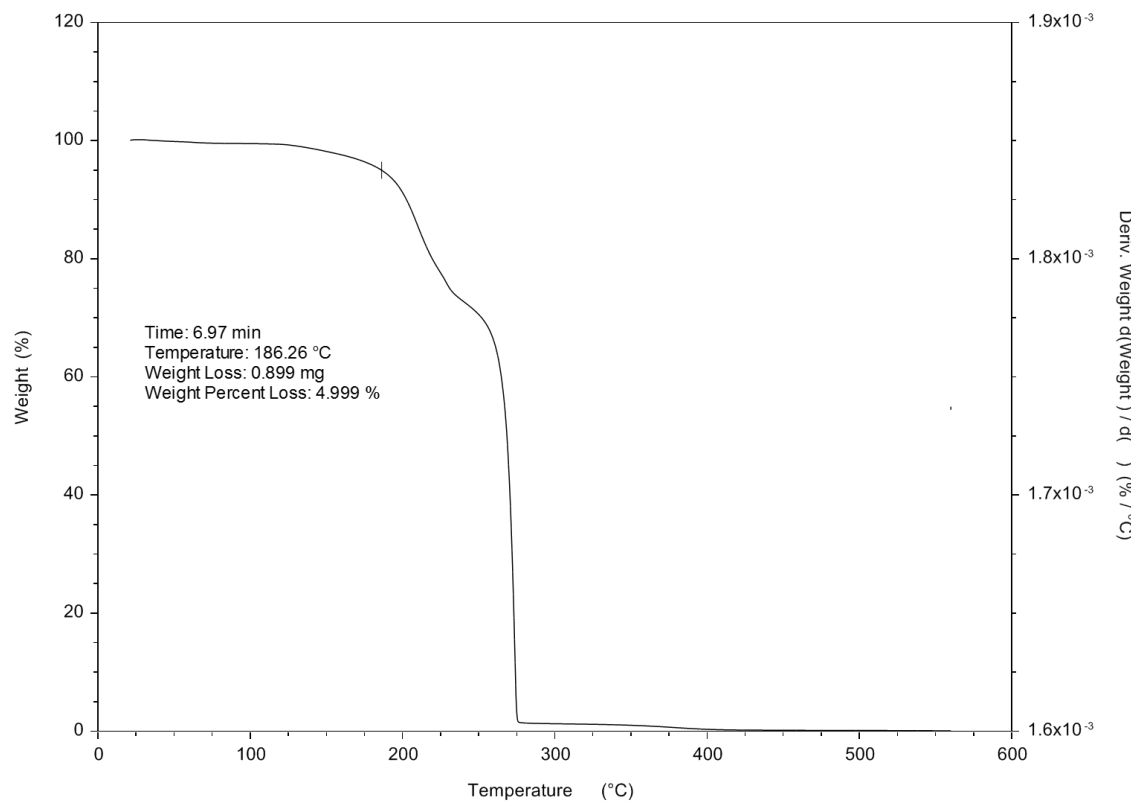
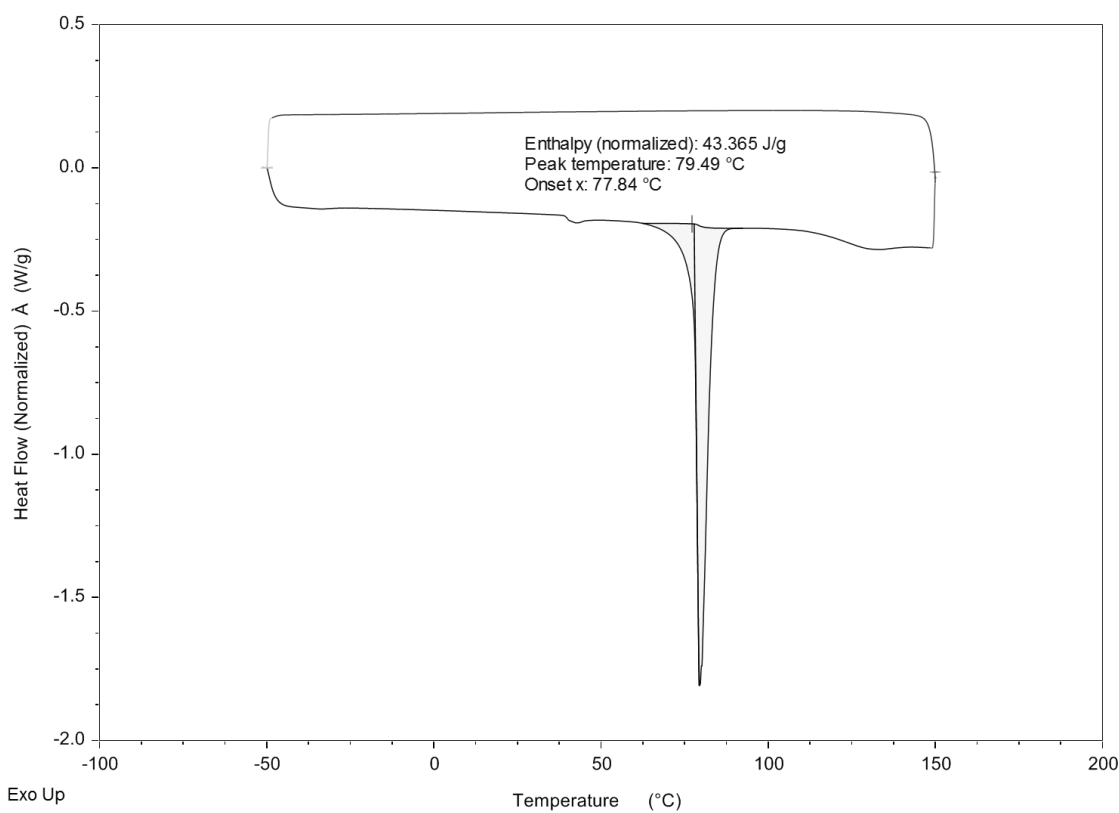


3e

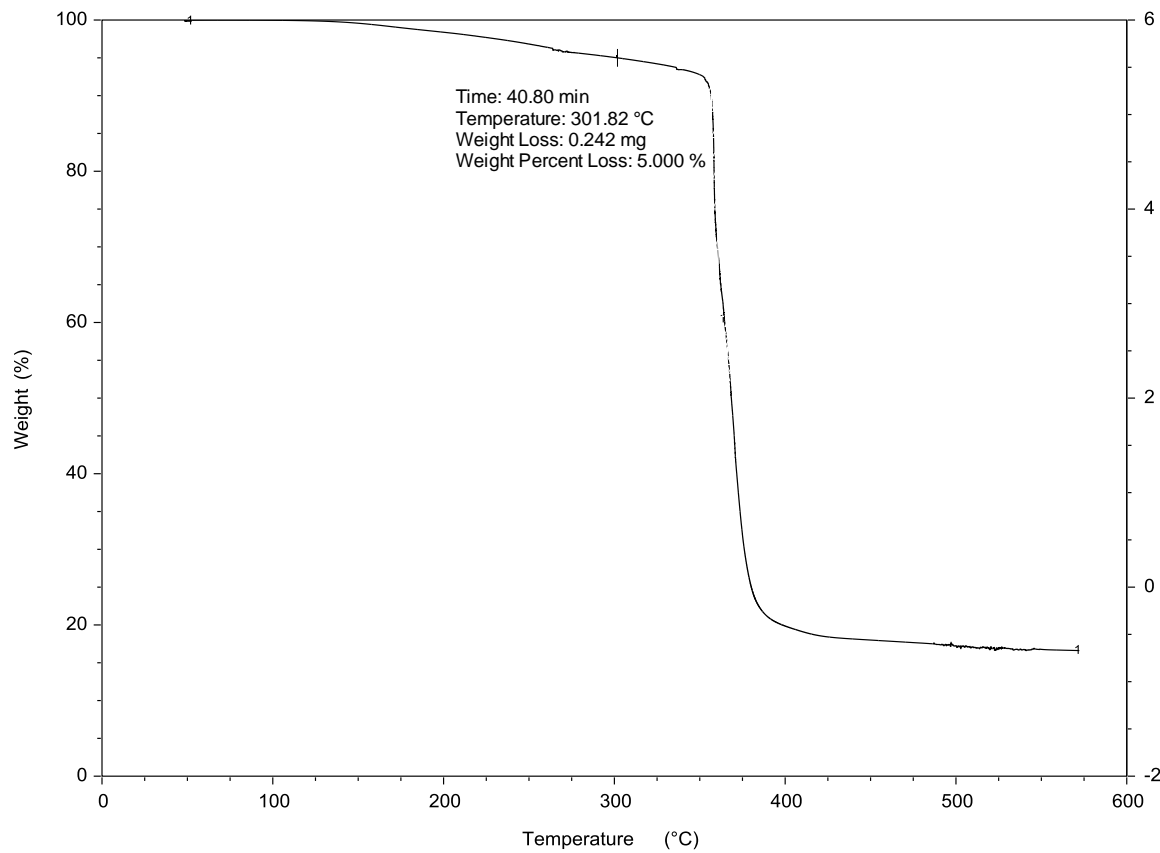
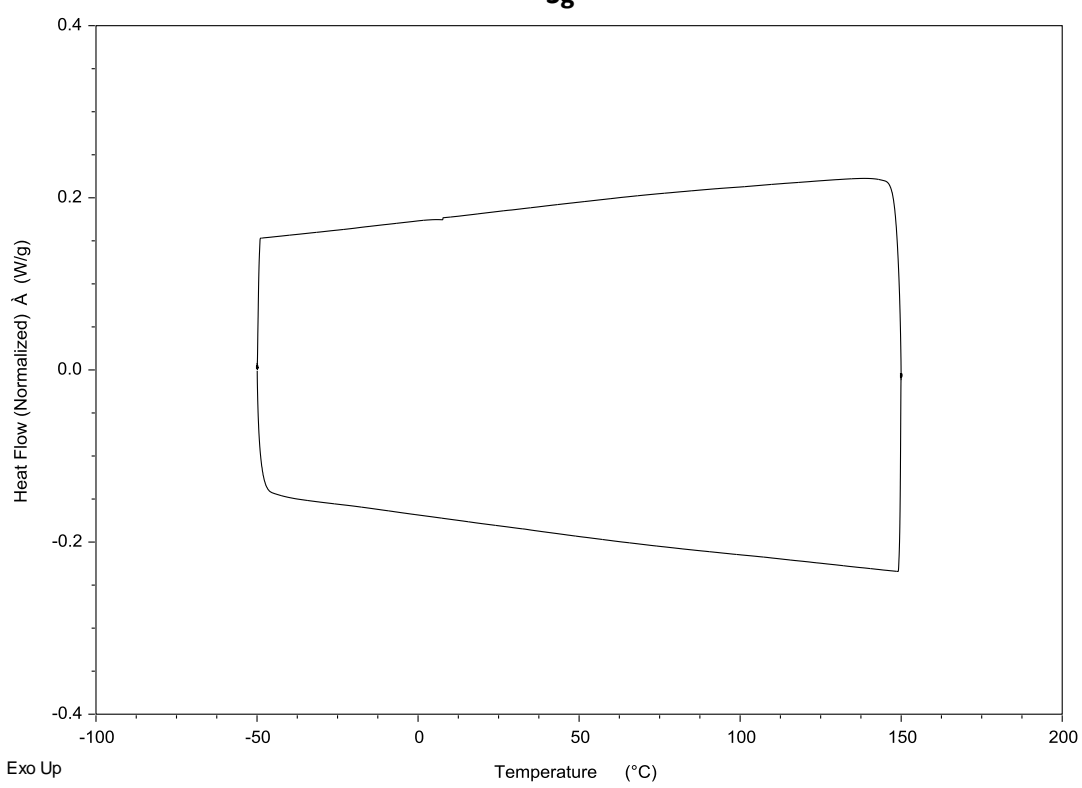


S40

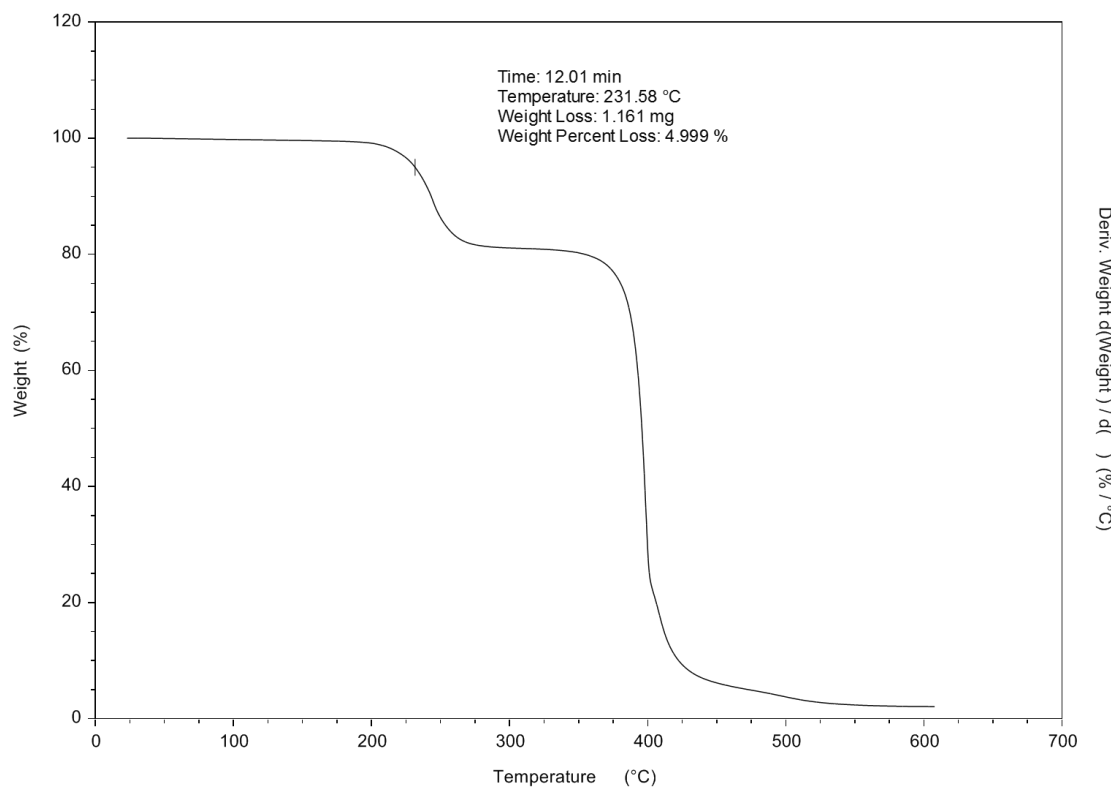
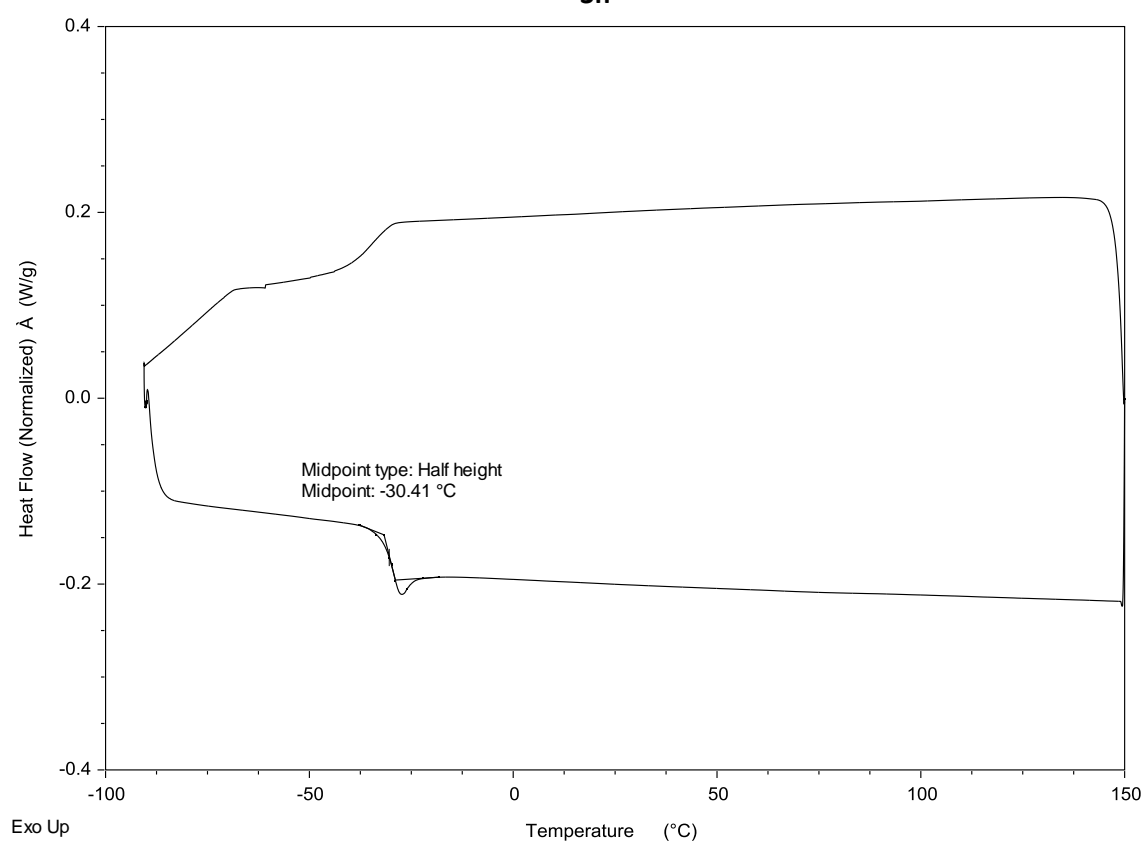
3f



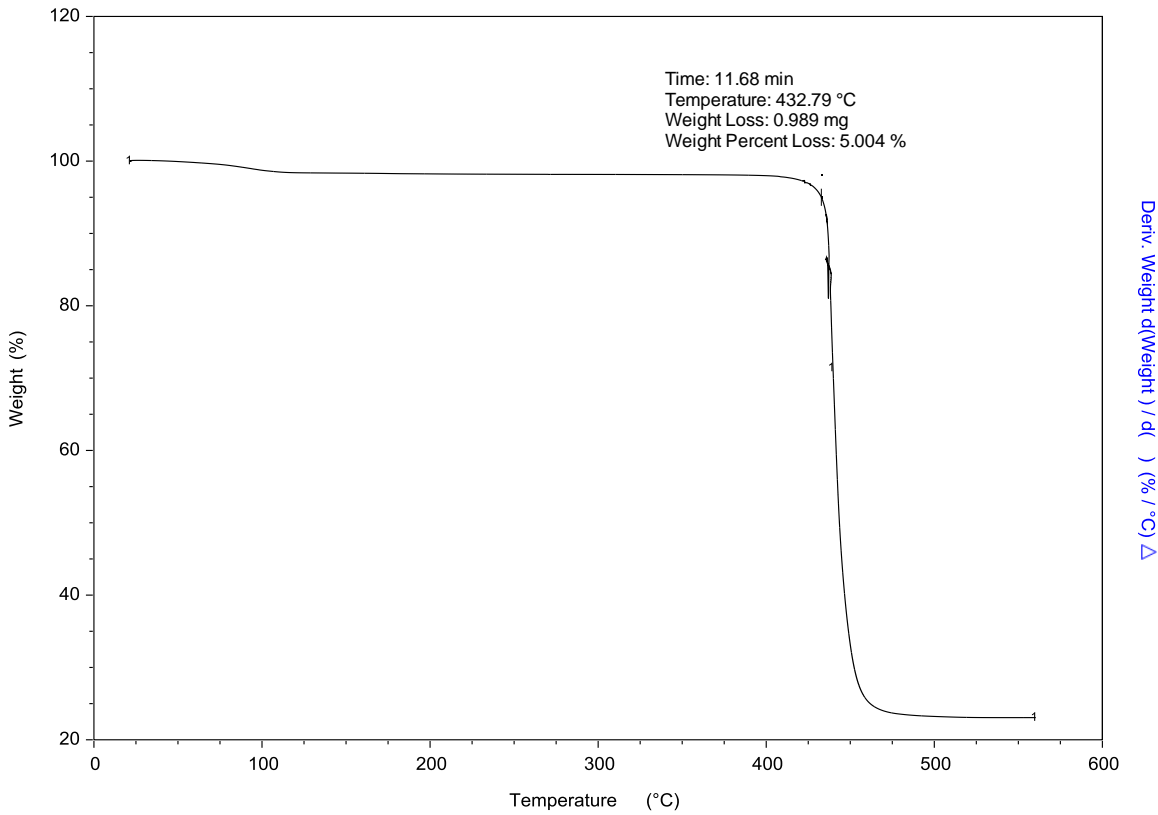
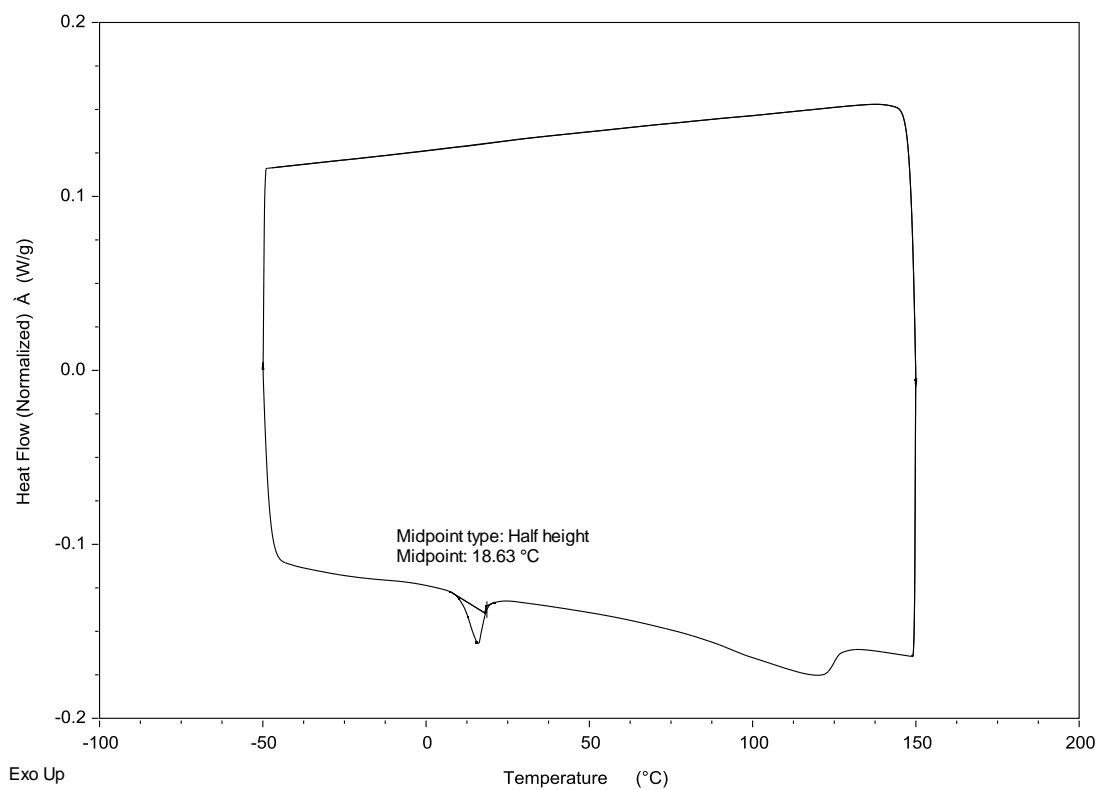
3g



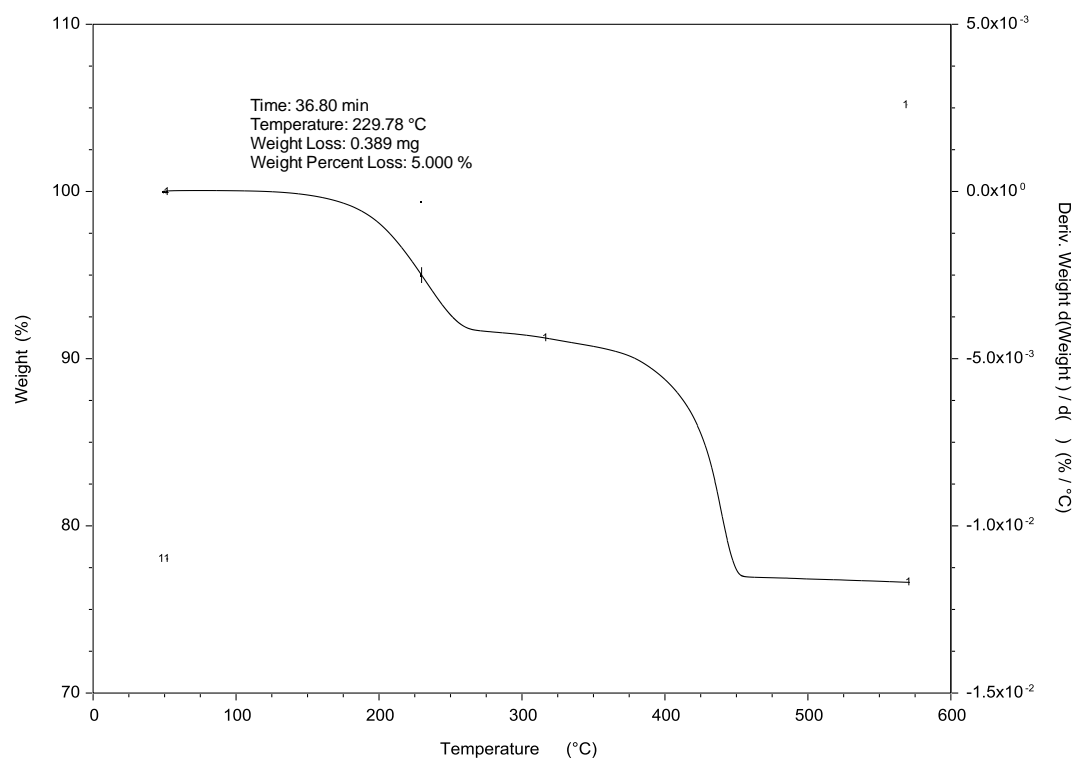
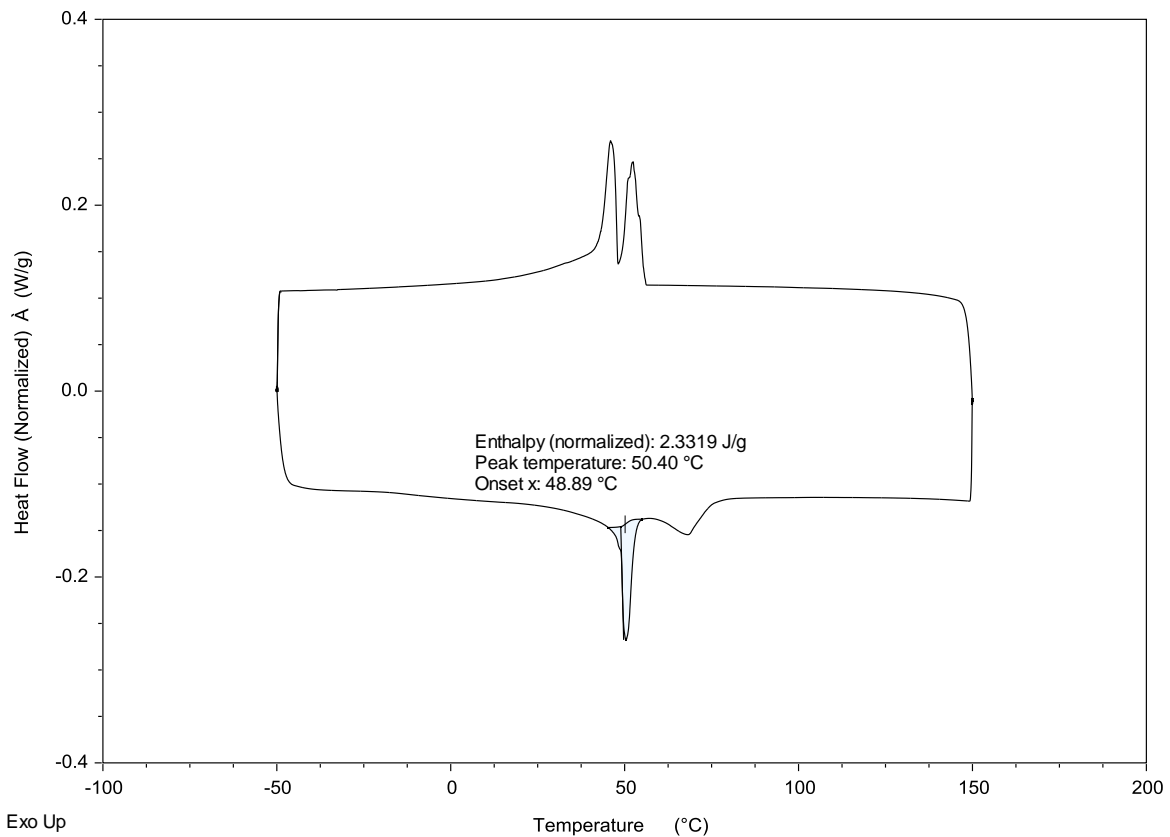
3h



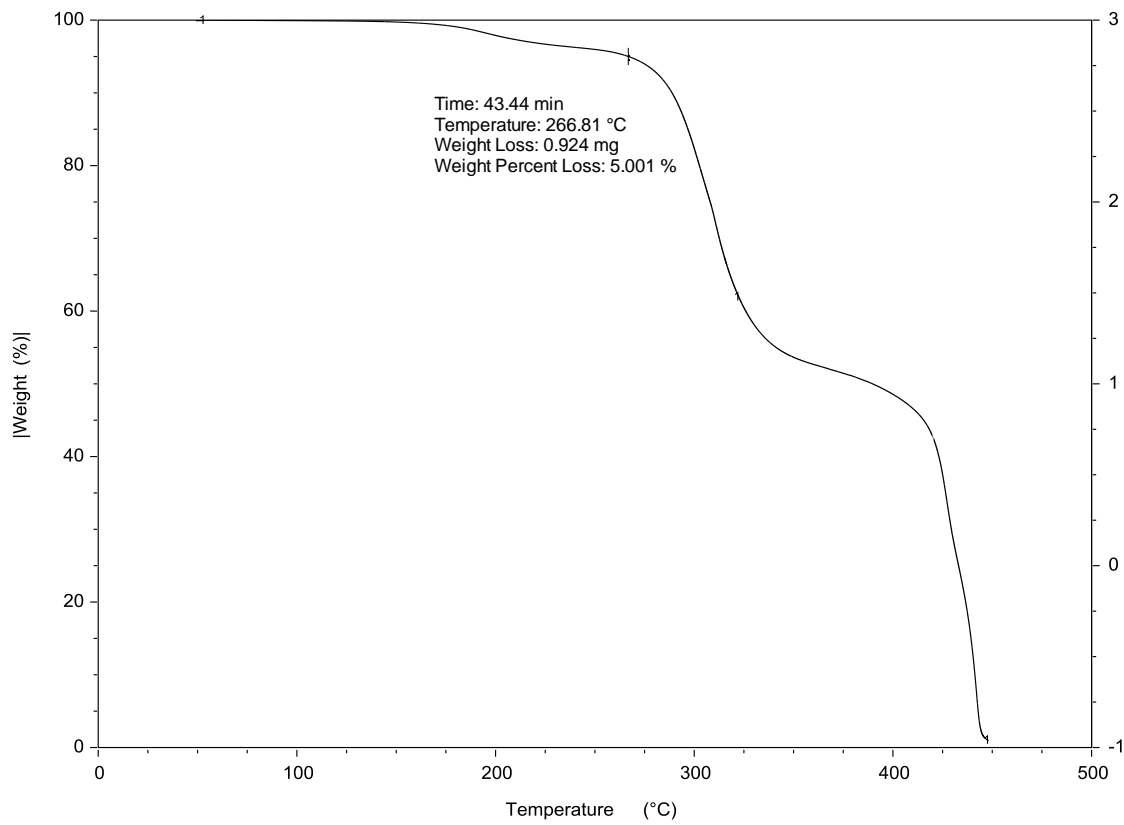
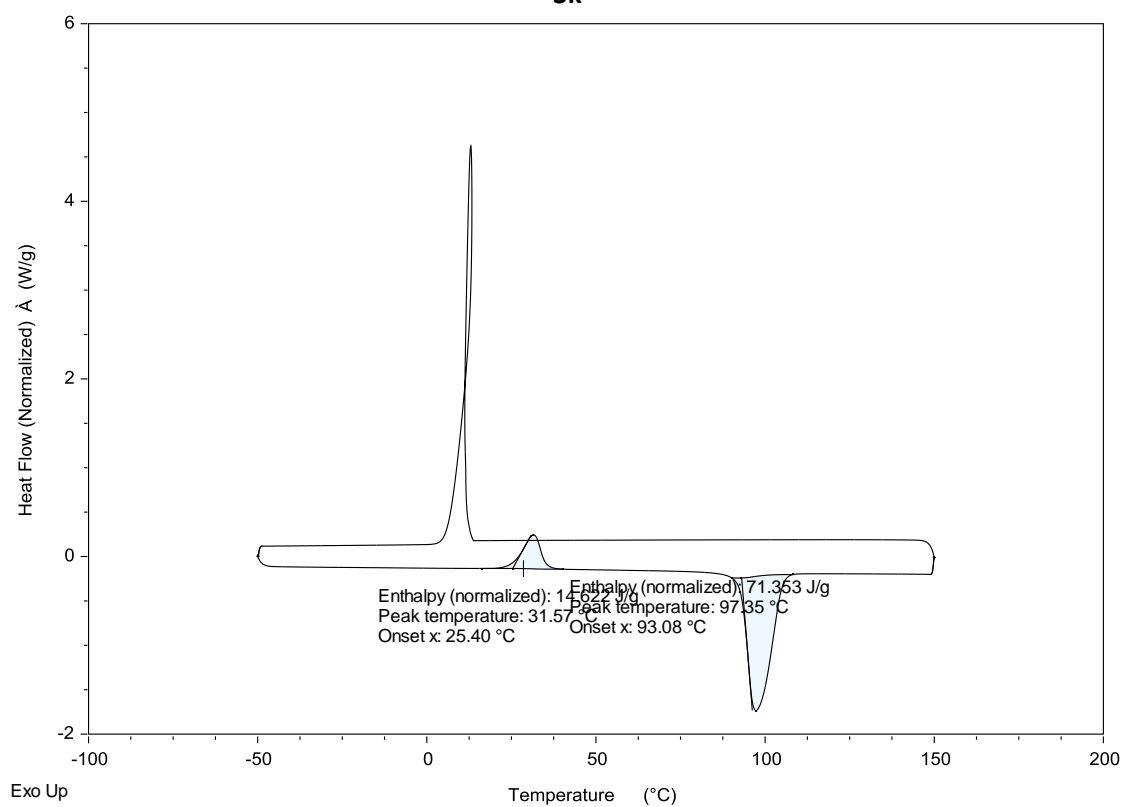
3i



3j



3k



3a – BETI

